International Journal of Concrete Structures and Materials

RESEARCH Open Access

Effect of Sugar Cane Bagasse Ash Incorporated as Viscosity Modifying Agent on Fresh, Microstructure and Mechanical Properties of Self-Compacting Concrete

Usman Amjad[1], Muhammad Sarir[2], Diyar Khan[3*], Inzimam Ul Haq[4*], Muhammad Wajahat Ali Khawaja[1] and Khalid Mahmood[1]

Abstract

The global construction industry faces a crucial challenge reconciling economic growth with environmental sustainability, notably due to the significant environmental impact of cement production, particularly in countries like Pakistan. As the demand for cement grows, so does the carbon footprint and environmental degradation, necessitating the exploration of sustainable alternatives like sugarcane bagasse ash (SBA), a byproduct of sugarcane processing, to mitigate these issues while also addressing rising costs in concrete production. Embracing SBA offers a promising avenue to alleviate environmental concerns and enhance the sustainability of the construction sector. This study investigated the SBA properties and effectiveness as a viscosity modifying agent (VMA) in self-compacting concrete (SCC), examining varying SBA content effects on fresh and hardened SCC properties. The hydration and microstructure properties were evaluated by using X-ray diffraction (XRD), scanning electron microscopy (SEM), and mercury intrusion porosimetry (MIP) to investigate SBA-based SCC. The results indicate that SBA has the potential to enhance mechanical and microstructural properties by possibly increasing the formation of Calcium Silicate Hydrate (CSH) gel. Adding 5% SBA demonstrated favorable fresh properties while incorporating up to 15% SBA showed improvements in compressive strength. Overall, adding SBA to cement manufacturing during clinkerization can reduce environmental pollution and lower production costs.

Keywords Sugarcane bagasse ash, Mechanical and microstructural properties, Self-compacting concrete

Journal information: ISSN 1976-0485/eISSN 2234-1315.

*Correspondence:
Diyar Khan
diyar.khan@polsl.pl
Inzimam Ul Haq
inzimamulhaq@kaist.ac.kr
[1] Department of Civil Engineering, Abasyn University, Peshawar, Pakistan
[2] Department of Civil Engineering, Faculty of Engineering and Technology, International Islamic University, Islamabad, Pakistan
[3] Doctoral School, Silesian University of Technology, Akademicka 2a, 44-100 Gliwice, Poland
[4] Department of Civil and Environmental Engineering, Korea Advanced Institute of Science and Technology (KAIST), 291 Daehak-ro, Yuseong-gu, Daejeon 34141, Republic of Korea

1 Introduction

Construction industry is paying a heavy price on a global level for being the ultimate sponsor of increase in the consumption of energy and materials, it has still managed to be the core element of globalized economic development (Anjos et al., 2020). Over the time, an incremented use of aggregate has been observed with an increase in the demand of cement as a binder (Gonzalez-Corominas et al., 2017; Soltanzadeh et al., 2018). Amidst the twenty-first century the extinction of the global nonrenewable resources has become a growing predicament (Hussain et al., 2020). The nonrenewable resources will be extinct in the near future as

the extraction, quarrying and mining of the resources from the environment will increase for the economic development. Being in limited quantity, the nonrenewable resources cannot be regenerated after they are extracted from mining (Ali et al., 2024; Ul Haq et al., 2022). Exposure of globe to an everlasting economic deterioration, namely, dust contamination, vegetation degradation, extinction of ecosystem, river damages, global warming and loss of biodiversity, is due to the unstoppable harvesting of the nonrenewable resources (Huntzinger & Eatmon, 2009; Hussain et al., 2020; Madlool et al., 2011; Mo et al., 2016; Valderrama et al., 2012).

Notoriously, affiliation of cement manufacturing has a pronounced role on environment. The main reasons responsible are CO_2 production during this process and lime stone and clays over extraction and exhaustion of these indigenous materials. Statistics indicate that energy released during the consumption of over 1-ton raw materials lies in the range of 2.93–6.28 GJ and it gives approximately 1 ton of CO_2 with surplus 65–141-kilowatt hours of electricity. As a result, climate changes have been triggered because of excessive strain on the global resources (Pacheco-Torgal, 2017; Stafford et al., 2016). Cement ovens, cement dryers and its preheaters need a lot of heat energy to operate as a considerable amount of fuel is required during the cement manufacturing process. The larger the volume of cement required; higher is the amount of energy consumed. In particularly, preliminary stages of cement manufacturing process contribute towards air pollution. It has been investigated earlier that during cement manufacturing process, 1 ton of cement contributes almost 0.8 tons of CO_2 to the environment and atmosphere (He et al., 2020). Another adverse effect of cement manufacturing is water pollution. Cement production phase is responsible for dust pollution which ultimately contributes to reduction of visibility and decreased air quality. The Centre of Disease Control and Prevention states that dust generated during cement manufacturing when drained off, it contaminates water and causes detrimental effects on well-being of human and even causes threat to animal safety. Ground water reservoirs and river water reservoirs are being contaminated due to wastewater runoff to atmosphere. Soil degradation problems caused by land human activities has been observed in those areas with increasing population, building and urbanization. Soil erosion is also caused as bad land control follows soil threats and water runoff through landscape preventing proper infiltration. Noise pollution is caused during the cement manufacturing process. Factors such as heavy machinery use for mixing of raw materials and clinker production, storage of the materials, complex gas noise, electrical magnetic noise and mechanical noise are they key sources of cement manufacturing process contributing to noise pollution in the surrounding environment (Mohamad et al., 2022).

Pakistan the world's 14th largest exporters of cement, ranked amongst the top 5 all over the world. In 2018 the cement production capacity of Pakistan reached 95 percent and with the contribution of China–Pakistan Economic Corridor the production level has increased since 2016. Due to the increase in carbon foot print caused by cement production, Pakistan is at 7th position amongst the most affected countries due to climate change according to Pakistan Economic Survey (2016–2017) (Zeb et al., 2018). A study was carried out on factors involved in the cost overrun of construction projects in the public sector area of Pakistan. Amongst other casual attributes, one of the prominent factors responsible for cost overrun in projects at Pakistan was the fluctuation and increase of prices of cement and other construction materials over time (Akram et al., 2017). India's consumption of cement reached to a value of 5% increase in 2019 as compared to 2018 when it utilized 460 million tons of cement, making India amongst the top 4 countries in the world to be contributing by 7% to the total carbon foot print across the globe.

This lead to believe that replacing cement with agricultural generated waste to a certain extent proves to be environment friendly (Basu et al., 2021a). Various researchers have investigated that as an alternative of cement, the use of sandstone is effective (Basu et al., 2021b). Silica-enriched agricultural by-products such as silica fume and rice husk ash, have also been used as supplementary cementitious materials in different studies (Basu et al., 2021b; Thomas et al., 2021a). Pozzolans being aluminous and siliceous not only are cementitious in nature but they also form CSH gel due to the hydration reaction analogous to cementitious products. Amongst such pozzolans is SBA which contains an abundant amount of silica (Thomas et al., 2021b). In addition, SBA incorporation in OPC affects both the fresh and hardened properties of concrete (Zhang et al., 2020a). SCA offers a dual benefit: it serves as a fuel supplement for energy-intensive processes and yields SBA as a by-product after burning. This by-product has the potential to reduce carbon emissions from the cement industry and can also be utilized as a cementing material in concrete (Ali et al., 2010). Furthermore, SBA incorporation into cement manufacturing during clinkerization can potentially mitigate environmental pollution and reduce production costs (Ali et al., 2009). In this study, the concept of life-cycle crack resistance was systematically investigated for internally cured concrete containing superabsorbent polymers (SAPs) using plate tests, ring tests, and fracture tests conducted at different ages. Micro

characteristics were analyzed using XRD, thermogravimetric analysis (TGA), MIP, and SEM tests. The findings contribute to the development of mix design guidelines and curing provisions aimed at promoting wider acceptance of SAPs for pavement concrete with enhanced crack resistance (Lyu et al., 2020). This study assessed the performance of concrete incorporating supplementary cementitious materials (SCMs) like fly ash, slag, and silica fume in frozen environments by varying SCM content, water-to-binder ratio, curing duration, freeze–thaw cycles, and salt-frost exposure. The investigation focused on chloride permeability and salt-frost resistance, evaluated through parameters such as RCM coefficient, scaling quantity per unit area (SQPUA), relative dynamic elastic modulus (RDEM), flexural strength, and microstructural analysis using TGA, XRD, SEM, and EDS techniques (Lyu et al., 2021).

In this study, SBA was employed as a VMA additive in SCC to enhance both its fresh and mechanical properties. Fresh properties were assessed through tests including slump flow, L-box, V funnel, and J-ring, while mechanical properties were determined via compressive strength tests. Furthermore, the hydration and microstructure characteristics of SBA-based SCC were analyzed using XRD, SEM, and MIP techniques.

1.1 Sugarcane Bagasse Ash and Self-Compacting Concrete

SBA is a residue obtained from burning of bagasse after the extraction of sugar. Bagasse cannot be landfilled as it causes detrimental degradation of environment (Deepika et al., 2017). Sugarcane mills need huge amount of electricity so as an alternative bagasse is also burnt for electricity generation in the sugar mills (Akkarapongtrakul et al., 2017). Bagasse ash is also a byproduct of sulco-alcohol industries as after extraction of sugar juice they are burnt and bagasse ash is formed (Zareei et al., 2018). A large amount of bagasse ash is produced due to these burning processes. A total of 26% bagasse ash at 50% of moisture content and 0.62% of residual ash can be produced by burning of 1 ton of bagasse ash. The production process is given in Fig. 1 (Akram et al., 2009; Xu et al., 2018).

Studies have been carried out that shows extensive burning, grinding or drying develops formidable properties for bagasse ash. The pozzolanic activity is enhanced for bagasse ash with this further burning, imparting higher surface area due to grinding where the availability of amorphous silica and lower carbon content imparts this improvement (Das et al., 2022). Characteristics of concrete improves when reactive silica in these ashes chemically reacts with $Ca(OH)_2$ during hydration reaction of cement which creates more CSH gels (Figueiredo & Pavía, 2020). In Pakistan, sugarcane production between 2016 and 2017 reached a record value of 71.37 million tons which exceeded the production value of 65.45 million tons for the years 2015–2016 (Khalil et al., 2021). Researchers are looking at potential alternatives to the common practice of dumping SBA in open areas, which has a negative impact on the ecosystem (Athira et al., 2020; Faria et al., 2012; Tripathy & Acharya, 2022). Literature shows that SBA as a supplementary cementitious material enhances mechanical properties of concrete mainly the compressive strength, tensile strength and elastic modulus (Cordeiro et al., 2019; Jagadesh et al., 2018). Another study carried out be Abbas. S et.al suggested that SBA is also effective in controlling the alkali silica reaction in reactive aggregate concrete (Abbas et al., 2020). Studies show that SBA also improves resistance against harmful effects of sulfate attack (Jagadesh et al., 2018), besides improving compressive strength and durability of SCC (Le et al., 2022).

A study has been carried out that burning of 1 ton of bagasse produces 24 kg of ash. Apart from co-generation boilers, the future of the application of SBA is in the manufacturing of SCC (Moretti et al., 2018). SCC has ability of high deformability which allows it an ability to compact on its own without the aid of the vibrator. Its high deformability and workability are achieved by the incorporation of viscosity modifying agents and high range water reducing agents which helps it to adjust in congested reinforcement. However, an increase in the

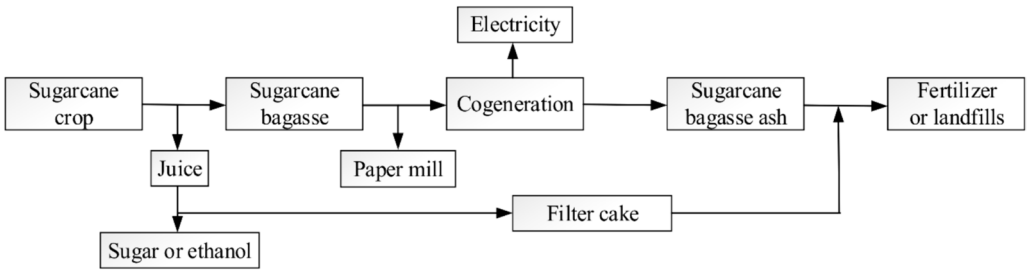

Fig. 1 Schematic diagram of bagasse ash

cost of production of SCC has been observed due to the use of these expensive chemicals (Das et al., 2022). Investigation on the properties of self levelling mortars was carried out by utilizing SBA as a partial replacement of Portland cement and it was found out that SBA improves the rheological, physical and mechanical behavior of mortars upon 25% of SBA replacement with Portland cement (Anjos et al., 2020). The high temperature effect on SCC containing high levels of SBA and metakaolin revealed that compared to SCC at room temperature, SCC containing up to 40% SBA and metakaolin shows less cracking and lower strength losses when heated (Larissa et al., 2020). Results obtained from SCC production with the use of fly ash utilizing SBA as fine aggregates indicated that comparable compressive strength and workability parameters are obtained at 60% of SBA. With 10% SBA, the maximum compressive strength was at 58.3 MPa. The use of bagasse ash to substitute up to 20% of the river sand improved the workability and hardening qualities of SCC. With 20% partial substitution of fine aggregate with bagasse ash, bagasse ash SCC mixes demonstrated improved workability, comparable strength, and reduced elastic modulus as compared to reference concrete (Muthadhi & Banupriya, 2021). A rheological investigation of the optimal dose of superplasticizer to cement ratio was used to construct self-compacting mortars with partial replacement of sand by SBA. The results showed that it was feasible to save up to 489 and 56 kg of sand and cement, respectively, to manufacture $1m^3$ of self-compacting mortar using SBA when the approximate replacement rate of sand by SBA was 40% (Molin Filho et al., 2019). Research on the viability of using SBA as a cement additive was conducted, and the results were compared to those obtained using rice husk ash. Up to 20% and 15% of cement replacement, respectively, the strength of bagasse ash blended concrete and rice husk ash blended concrete is greater than that of the control concrete. Including either bagasse ash or rice husk ash into concrete at the optimal replacement levels improved the material's resistance to chloride, water, and air permeability (Jittin et al., 2021a). Examining the properties of bagasse ash and its long-term application as a concrete additive, Tripathi and Acharya found that processed SBA has superior properties to its unprocessed counterpart at an optimal replacement of 20%, making it an excellent choice for use in both binder and filler applications (Tripathy & Acharya, 2022).

According to the literature reviewed bagasse ash has been used in SCC as a pozzolan, SCM and as a replacement of aggregate. The amount of work done on the possibility of bagasse ash usage as an ecofriendly VMA in SCC is yet to be investigated. The aim of this research is to investigate the possibility of SBA to be used as a replacement for expensive viscosity modifying agent in SCC and subsequently to study some fresh and hardened properties of SCC along with a characterization study through XRD, SEM and MIP to deduce conclusion about the optimum use of the SBA in SCC for this purpose.

Table 1 Physical properties of OPC

Cement brand	Cement	ASTM Standard
Cement type	Type 1 (OPC)	C-150
Average particle diameter (mm)	< 33	C-204
Consistency (%)	31	C-187
Initial setting time (min)	96	C-191
Final setting time (min)	198	C-191
Density (g/cm3)	3.15	C-77
Compressive strength at 28 days (MPa)	38	C-150

Table 2 Oxide composition of OPC and bagasse ash

%Oxide	Cement	Bagasse ash
SiO_2	19.00	62.44
Al_2O_3	09.87	06.74
Fe_2O_3	03.46	05.77
CaO	60.00	06.16
MgO	01.63	02.97
SO_3	02.63	00.72
Na_2O	00.84	03.15
K_2O	01.19	06.87

2 Experimental Program

2.1 Materials and Mixture

2.1.1 Cement

Cement used was Ordinary Portland Cement (OPC), Type 1 as per standard of ASTM C150 in the fresh state (ASTM C150 & C150M-20, 2020). The physical properties of OPC were evaluated in materials laboratory of Abasyn University, Peshawar, as shown in Table 1. The oxide composition of OPC in comparison with bagasse ash is shown in Table 2.

2.1.2 Aggregates

Natural sand as fine aggregate from the quarry site at Nizampur, Khairabad and with an upper limit of 20mm coarse aggregate from the quarry site at Bassay, Peshawar was used. Nominal sizes of 10mm and 20mm of coarse aggregate were mixed in 1:1 by weight. Crushed limestone (quarry site at Bassay, Peshawar) having upper bound of 20 mm was used as coarse aggregate. Two different nominal sizes were mixed, namely, 10 mm and 20 mm. The mixing ratio of 10 mm to 20 mm aggregates

was 1:1 by weight The sieve analysis of fine and coarse aggregate was carried out as per ASTM C136 (ASTM, 2019). The sieve analysis of aggregates were compared with ASTM C33 (Astm, 2003). The sieve analysis of fine and coarse aggregate in comparison with ASTM C33 and their physical properties are shown in Table 3. Figs. 2 and 3 show the sieve analysis graph for coarse and fine aggregates, respectively.

2.1.3 Superplasticizers

To provide higher workability and placing ability, a traditional high range water reduction additive called Ultra Super Plast 310 (2% by weight of binder for control concrete and blended mixes) was utilized. Sika Viscocrete-20HE, a commercially available brand of superplasticizer for viscosity, was used to create the control concrete ("SIka Viscocrete 20HE", Sika® ViscoCrete®-20 HE High Range Water Reducer / Superplasticiser xxxx; Alberti et al., 2020).

2.1.4 Sugarcane Bagasse Ash

The SBA was obtained from sugar mills located at Khazana near Peshawar, Khyber Pakhtunkhwa. For the grinding process, a Los Angeles Abrasion Machine was used

Table 3 Sieve analysis and physical properties of aggregates

Sieve No.	Fine aggregate sample Weight = 1152.23 gm	Coarse aggregate sample Weight = 3984 gm	ASTM C 33
	Retained weight (gm)	Retained weight (gm)	Percentage
3/4	0	235	90 to 100
1/2	0	1143	–
3/8	0	482	20 to 55
No. 4	0	1880	0 to 10
No. 8	0	0	
No. 16	334.38	0	50 to 85
No. 30	213.62	0	25 to 60
No. 50	477.94	0	5 to 30
No. 100	88.84	0	0 to 10
No. 200	0	0	
Pan	37.47	244	–
Fineness modulus	2.62		–
Dry rodded unit weight (kg/m^3)	1953.54	1529.28	–
Bulk specific gravity (SSD)[a]	2.671	2.678	–
Absorption (%)	1.65	1.07	–

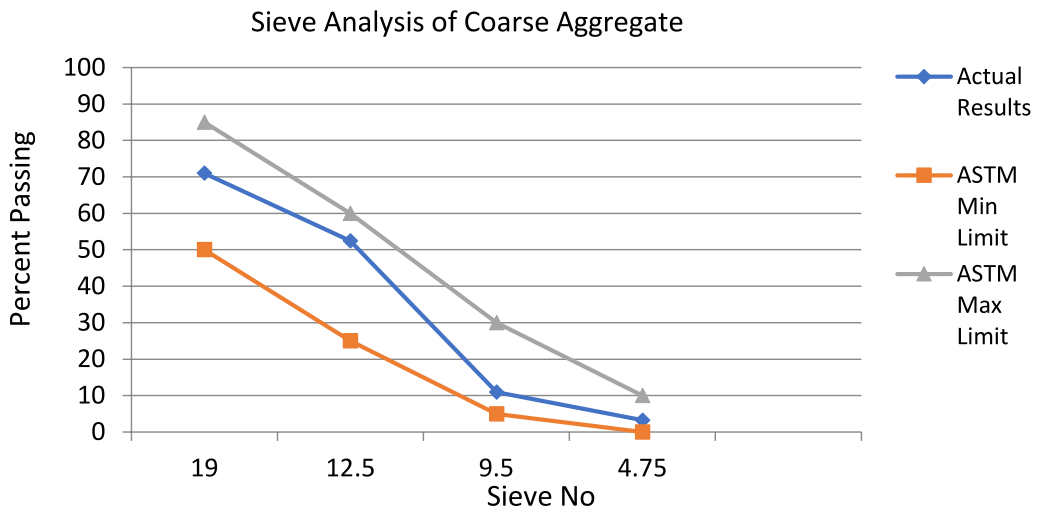

Fig. 2 Sieve analysis of coarse aggregate

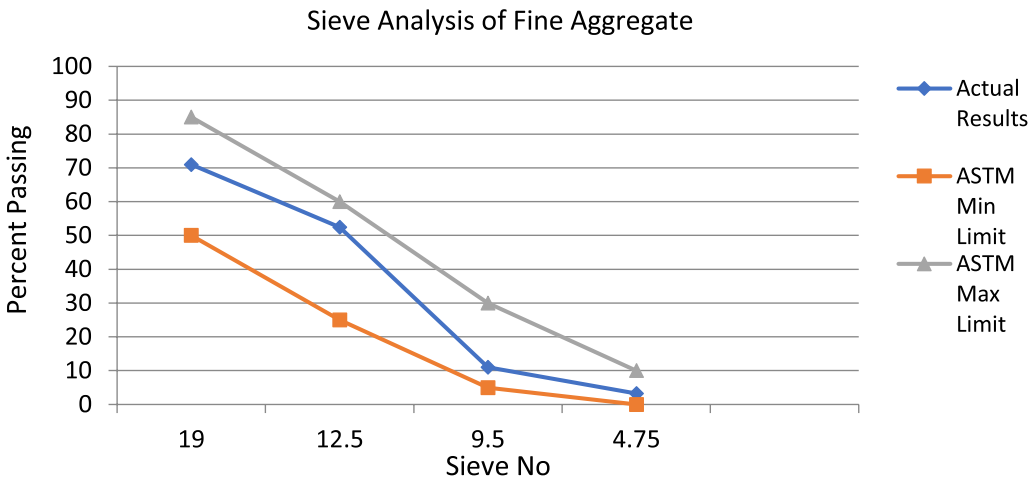

Fig. 3 Sieve analysis of coarse aggregate

(Astm, 2008). Two thousand five hundred rotations were used to grind up bagasse ash. After the ash had cooled, it was sieved through a No. 100 mesh screen. The ash that was retained was discarded, and the ash that passed through the sieve was crushed again for a total of 500 rotations. Ash that made it past sieve no. 200 was collected for testing. All the step-by-step procedure is shown in Fig. 4. The ash was kept in a dry area after being

Fig. 4 Sieve analysis of coarse aggregate

sealed in a polythene bag. The amount of ash needed for the mix samples was retrieved from this method, as predicted by the mix design. Cement with 5%, 10%, 15%, and 20% bagasse ash by weight was utilized. Each proportion was then added to the 2% superplasticizer mixture.

2.1.5 Mix Proportion and Preparation of Specimens

SBA is used as an additive and as a VMA at various levels (Anjos et al., 2020; Hasnain et al., 2021). Cement with "5, 10, 15, and 20" percent bagasse ash by weight was utilized. Each proportion was then added to the 2% superplasticizer mixture. ACI 211.1-91 (Committee & "Standard practice for selecting proportions for normal, heavyweight & mass concrete", 1991) was used for the proportioning of SCC control and bagasse ash mixes. The names of the specimens were referred to by their abbreviations, such as SCC-CM and SCC-5B, etc. When referring to SCC-CM, "SCC" refers to Self-Compacting Concrete, while "CM" refers to the control mix that is produced by mixing it with VMA. In the same way, "5B" in SCC-5B refers to the percent dose of SBA that is applied relative to the total weight of the binder. Fig. 5 shows the samples for compressive strength with prospering capping.

Five different mixtures, including one control mix and four mixes with various amounts of SBA, were cast. Table 4 provides the mixed design matrix for SCC.

Each batch of concrete was used to cast nine cylinders measuring 150 mm by 300 mm as per ASTM C39 (Astm, 2005). These cylinders, which were cast without vibration, were utilized to determine the 7, 28, and 56 day strengths of the material. After the casting process, every molded specimen was placed under a covering made of plastic sheets for a period of 24–8 h. Following 1 day, the specimens were removed from the cylinder molds and transferred to wet curing tubs, where they remained at 25°C until they were required for testing.

Fig. 5 Samples for compressive strength with prospering capping

2.2 Testing Plan

2.2.1 Fresh State Tests

The slump flow, L-Box test, V-Funnel at $T_{5\,min}$ test, and V funnel (6–12 s) test were performed in accordance with EFNARC Guidelines (Efnarc, 2002). The J ring test was performed in accordance with ASTM C1621 (Standard, 2009) to investigate the impact of SBA as VMA on the SCC characteristics in the fresh state.

2.2.2 Hardened State Tests

2.2.2.1 Microstructural Investigation X-Ray Diffraction: X-ray diffraction method opted by previous researchers (Bibi et al., 2020; Chopra & Siddique, 2015; Diab et al., 2016; Khater, 2013) was also used in this study. From prism samples of 4 cm x 4 cm × 16 cm that were fractured in flexure, specimen fragments of roughly 2–4 mm size were produced. With the help of iso-propanol and acetone, the hydration was stopped. The specimen pieces were then ground to a size of between 5 and 30 microns.

Table 4 SCC mix design proportion matrix

SBA (%)	Cement (kg/m^3)	Fine aggregate (kg/m^3)	Coarse aggregate (kg/m^3)	Bagasse ash (kg/m^3)	Super plasticizer (% by weight of binder)	Viscosity modifying agent (% by weight of binder)
SCC-CM	500	875	750	–	2	2
SCC-5B	500	963	750	25	2	–
SCC-10B	500	963	750	50	2	–
SCC-15B	500	963	750	75	2	–
SCC-20B	500	963	750	100	2	–

For the XRD investigation, 5–10 g of the powder were employed. Step size: 0.013°, counting time per step: 29 s, and angular range: 5–90° (2 Theta) were among the measurement parameters. X-ray tube power is 40 kV/40 mA, the anode is Cu, and the radiation is Cu K α.

Scanning Electron Microscopy: Scanning electron microscopy (SEM) used by previous researchers (Bibi et al., 2020; Zhang et al., 2020b; Zhang et al., 2020b) was used in this study in accordance with ASTM C1723-16 (ASTM C, 2016). In addition to the pictures produced by the SEM, qualitative chemical composition and X-ray microanalysis carried out by energy-dispersive X-ray spectroscopy (EDX) (Ameri et al., 2019; Hasnain et al., 2021; Jain et al., 2022) were acquired for each sample. After isopropanol and acetone were used to stop the hydration process, the specimens of powdered secondary raw materials and samples of self-compacting paste were put through a series of tests to see how they changed over time. The goal was to investigate the microstructure, morphology, and hydration products at different ages of the material.

Mercury Intrusion Porosimetry: Mercury intrusion porosimetry (MIP) for the pore size distribution as done by previous researchers (Sidiq et al., 2020; Tibbetts et al., 2020) was carried out in accordance with ASTM D4404 (ASTM D4404, 2004) The Pascal 440 mercury intrusion porosimeter was used to conduct the investigation on pore size distribution. For flexure and compression tests, samples made from previously cast prisms were prepared. After being compressed, these prisms were fractured with a chisel and a hammer to a size of 5 mm. Then, these samples were dipped in an iso-propanol and acetone solution to terminate the hydration process. The samples were subjected to controlled incremental pressure up to 400 MPa after drying. Pascal 440 Porosimeter was used to capture all pressure measurements as well as mercury intrusion volume and pore radii. The surface tension of mercury was 480 dyne/cm, and the contact angle between mercy and the pore wall was 140°.

2.2.2.2 Mechanical Tests Compressive Strength test was performed on a 150 mm diameter and 300 mm height cylinder in accordance with ASTM C39 (Astm, 2005). The cylindrical samples for the compressive strength test are shown in Fig. 5. Density of hardened concrete cylinders was calculated as per ASTM C642 (Standard, 2006).

3 Results and Discussion

3.1 Slump Flow Test

Fig. 6 shows the slump flow test results. The SCC containing SBA flowability range of the SCC containing SBA was from 313 to 675 mm as per the EFNARC Guidelines. The control SCC showed the highest flow. However, as the SBA proportion was added into SCC, the flowability gradually decreased as the SBA increased. It was due to the high surface area as well as the various particle shapes

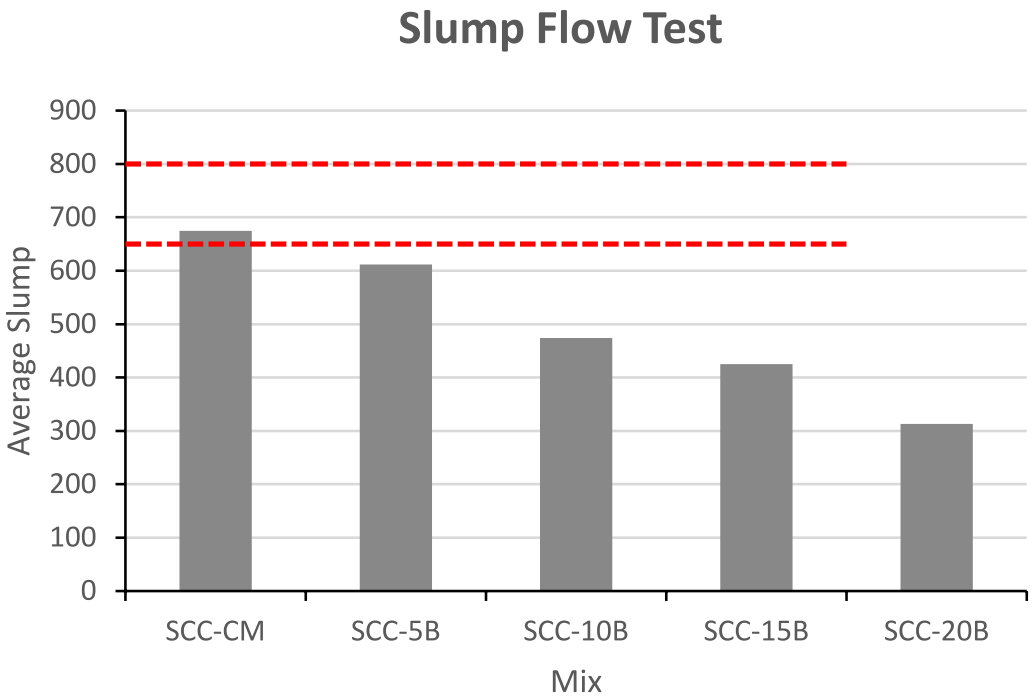

Fig. 6 Slump flow test results

that increased the flow fraction and led to a reduction in the flow table value (Saad Agwa et al., 2022). According to the EFNARC Guidelines, the control mix of SCC and the mix containing 5% SBA results followed the SCC limit. It is evident from the findings that despite maintaining the superplasticizer value at the same level, the values of slump flow continued to decrease as SBA was gradually added to each of the blended mixtures.

3.2 L-Box Test

Fig. 7 depicts the L-box test results. Similar to the flow table test results, L-box results were observed in the same manner. The control mix showed the highest L-box value of 0.9 with a gradual decrease occurring as the SBA proportioned added. The lowest L-box value of 0.7 was shown by SCC-10B. According to the EFNARC Guidelines, the lowest blocking ratio for the SCC should be more than 0.8. The values of the results ranged from 0.9 to 0.7 for the first three mixes (SCC-CM, SCC-5B, and SCC-10B), and these mixes crossed the steel bars without any obstruction. The preceding two mixtures, SCC-15B and SCC20B, both had a high viscosity and caused the assembly to become clogged. Therefore, from the result, it was concluded that the SCC-5B can be used as a cementing material in terms of flow only to provide the acceptable flow value for the required application.

3.3 V-Funnel at $T_{5\ minutes}$ Test

The findings of the V-funnel $T_{5minutes}$ test, as shown in Fig. 8. In general, from the results, it was observed that the addition of SBA in SCC mixes was passed from the funnel without any restriction. Both SCC-5B and SCC-10B showed results that were acceptable according to the EFNARC guidelines. The mixes SCC-15B and SCC-20B were outside of the EFNARC acceptable range of values.

3.4 V-Funnel at $T_{(6–12\ s)}$ Test

Fig. 9 depicts the V-Funnel at $T_{(6–12\ s)}$ test results. Similar to the V-Funnel at $T_{5\ min}$ test results, the same results were observed in 6–12 s time. Both SCC-CM and SCC-5B displayed values that were relatively close to those of the EFNARC range. The mix proportions SCC-10B, SCC-15B, and SCC-20B were all outside of the SCC acceptable range of values. According to the findings, a greater quantity of SBA was added to each blended mix, which resulted in an increase in the concrete viscosity and reduced the flowability.

3.5 J-Ring Test

The J-ring test results are shown in Fig. 10. From the results, it was determined that as the SBA dosage increased in SCC, the J-ring time increased because of the high viscosity that led to an increase in the obstruction in the steel bars. The control mix showed 15 s and as the SBA proportion increased, there was a linear increase in the time taken by the SCC up to 55 s.

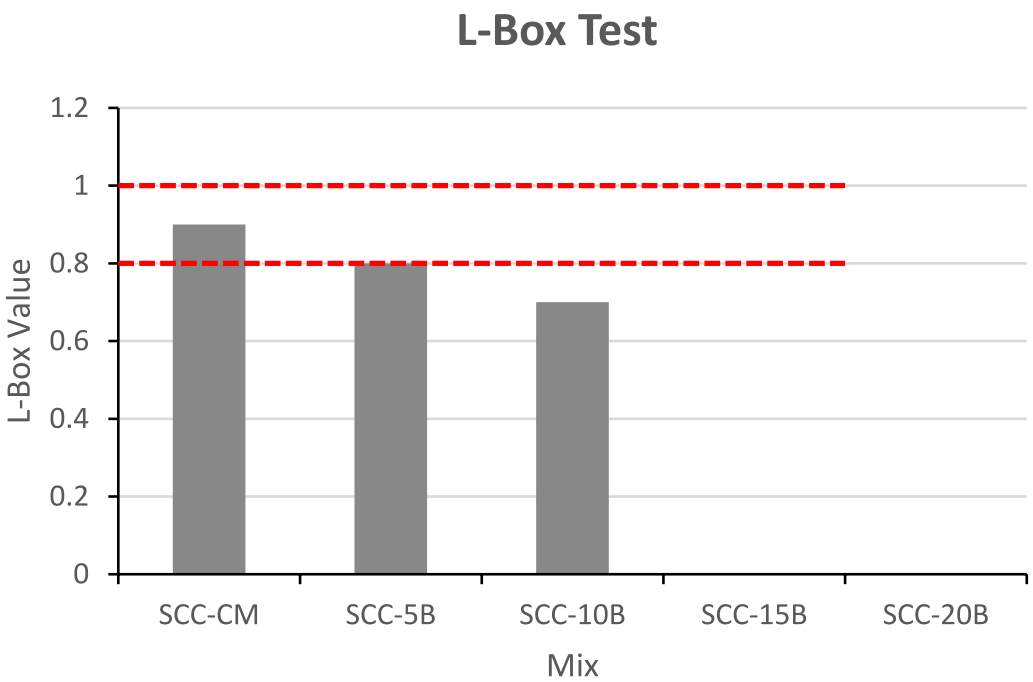

Fig. 7 L-box test results

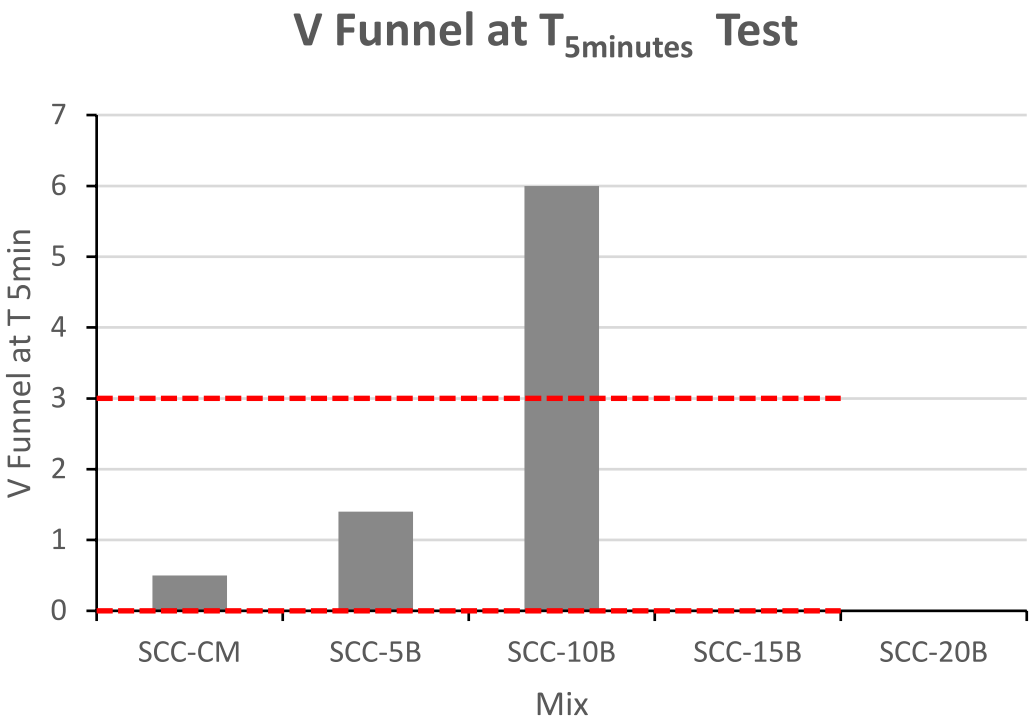

Fig. 8 V-funnel at $T_{5minutes}$ test

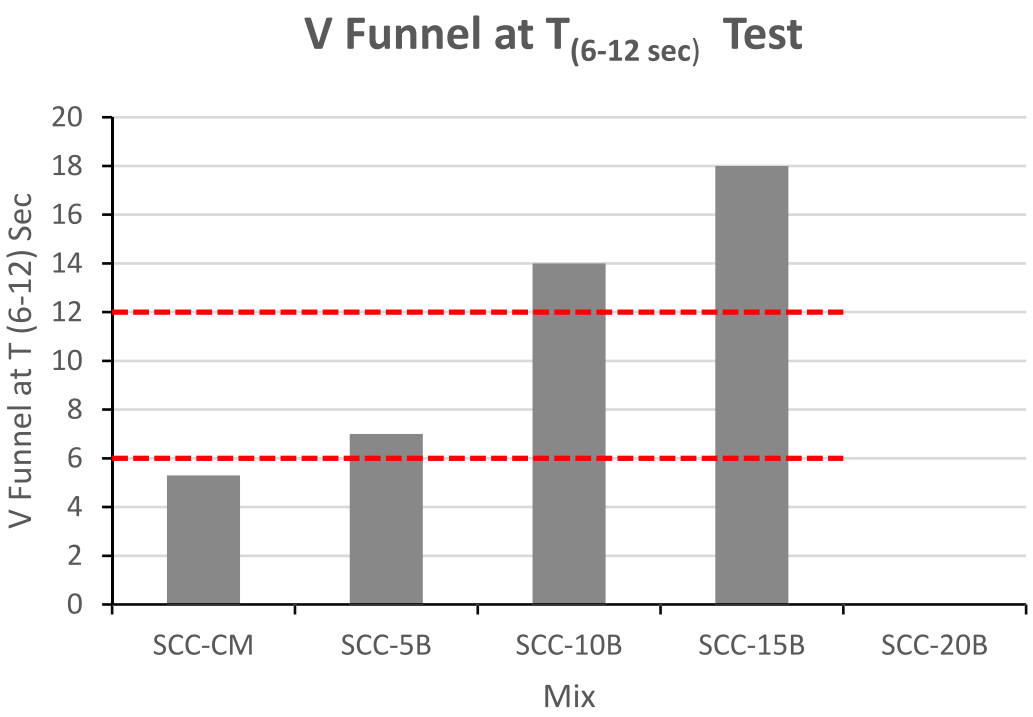

Fig. 9 V-funnel at $T_{(6-12\ s)}$ test

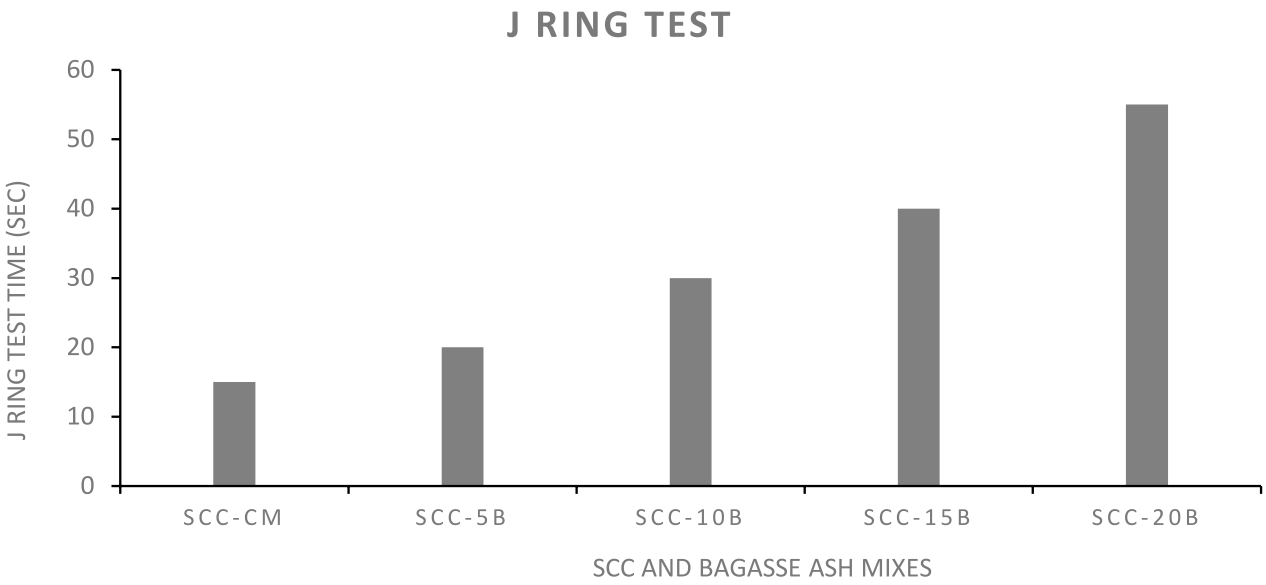

Fig. 10 J ring test results

3.6 X-Ray Diffraction

Figs. 11, 12, 13, 14, 15, 16, 17 show the XRD results of the control and SBA mixes of SCC after 1 day and 7 days of curing. A qualitative investigation was performed on SCC-10B and SCC-15B for SBA, in addition to all SCP formulations. According to the findings, the cement sample from Askari has several phases that are characteristic of OPC, including alite (60%), belite (17%), ferrite (11%), aluminate (7%), and anhydrite (4%). The sample of SBA consists primarily of amorphous material, with small traces of the mineral's quartz and cristobalite present. In addition to it, there is a hint of a phase that might be feldspar (Albite). Alite, Belite, Ferrite, Quartz, Portlandite, and Ettringite are some of the common phases that might be found in a hydrating OPC-based mortar, which can be found in the SCC-CM, 1D sample. Alite, Belite, Ferrite, Quartz, Portlandite, and Ettringite are all present in the SCC-10B, 1D sample, in addition to Cristobalite (Thomas et al., 2021c). Alite, Belite, Ferrite, Quartz, Portlandite, and Ettringite are the phases that may be found in the SCC-10B, 1D sample. At the age of 7 days, the identical phase assemblage can be detected in all the self-compacting paste formulation samples that have been collected. Ettringite and Portlandite are the hydrated components of the formulations, whereas Alite, Belite, and Quartz are the non-hydrated remainders of the formulations. The addition of SBA can potentially increase the formation of CSH gel due to the rich silica content and can react with portlandite to increase the strength as well as make denser the microstructure (Thomas et al., 2021c). In OPC, the main hydration product that increases both the strength and durability like CSH can be enhanced using SBA. The pozzolanic reaction mechanism can be occurred by using SBA and it reaction rate depends on the optimum proportion of SBA (Yadav et al., 2020).

3.7 Scanning Electron Microscopy

Figs. 18, 19, 20, 21, 22, 23 show SEM images of SCC-CM, SCC-10B, and SCC-15B after 1 and 7 days curing, coupled with the results of dispersive X-ray spectroscopy (EDAX) investigation. From the results, it was observed that in each mix composition, there was the formation of ettringite crystals in the form of needle-like cubic structures, as well as the creation of massive hexagonal calcium hydroxide crystals. The CSH gel that does not contain a well-defined crystalline structure may also be seen in the cementitious mix. The formation of CSH can densify the microstructure, potentially enhancing the strength and durability of SCC by using SBA (Thomas et al., 2021c). This increase in CSH gel formation may result from the pozzolanic reaction between the silica in SBA and portlandite, a primary hydration product of OPC (Channa et al., 2022). Zang et al. (2020a), investigated SBA as a potential supplementary cementitious material (SCM), demonstrating its ability to enhance strength and durability properties through pozzolanic reactions. Nevertheless, the pozzolanic reaction of SBA is primarily affected by the physical and chemical properties, along with its calcination temperature (Jittin et al., 2021b; Memon et al., 2022). Alite, Belite, Ferrite, Aluminate and Anhydrite are some of the usual OPC phases found in the Askari cement sample, as shown by the results. There is mostly amorphous material in the SBA mix proportion, with some smaller amounts of Quartz

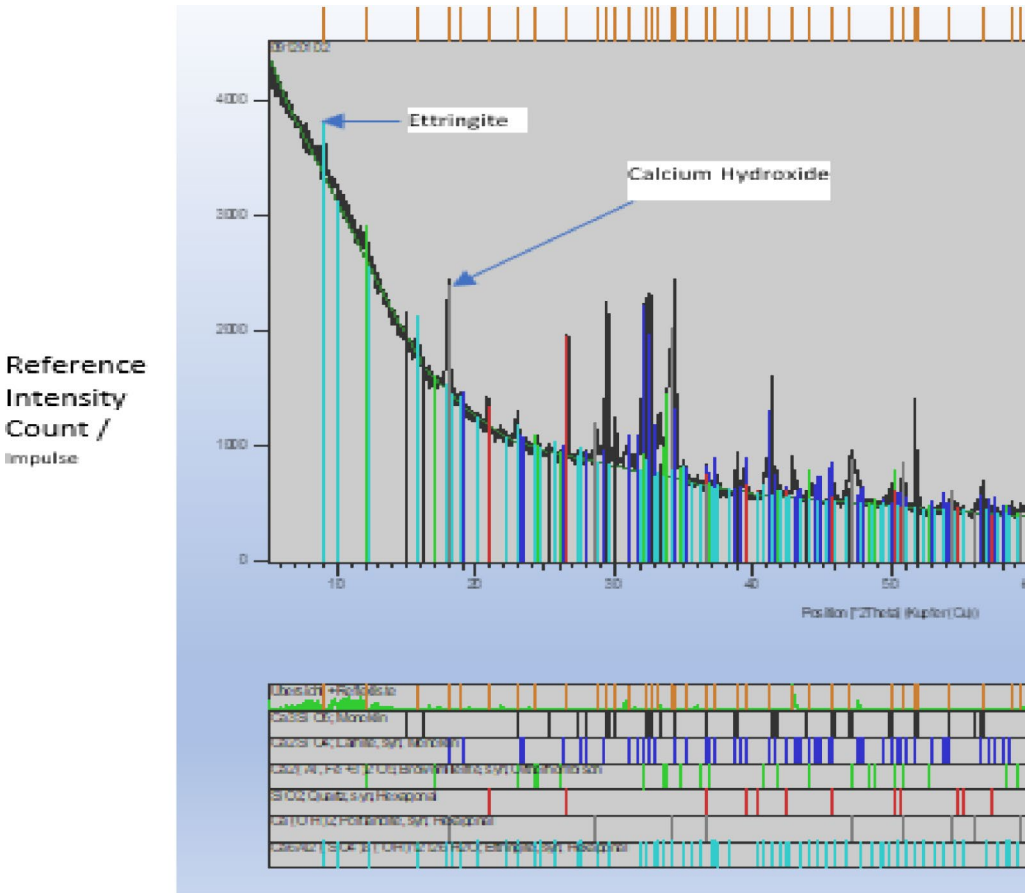

Fig. 11 XRD examination of the SCC-control mix sample at the age of 1 day, identifying the following main phases: alite, belite, ferrite, quartz, and ettringite

and Cristobalite. In addition, a phase that may be feldspar (Albite) has also been detected. The SCC10B, 1D sample includes Cristobalite in addition to Alite, Belite, Ferrite, Quartz, Portlandite, and Ettringite. Alite, Belite, Ferrite, Quartz, Portlandite, and Ettringite are all present in the SCC10B, 1D sample. At 7 days, the same phase assemblage is present in all samples of self-compacting paste formulations. The hydrated components of the formulas are ettringite and portlandite, whereas the non-hydrated components are alite, belite, and quartz.

3.8 Mercury Intrusion Porosimetry

Mercury Intrusion Porosimetry was only performed up to a maximum of 7 days. The samples' average pore size radius and total porosity are shown in Figs. 24 and 25, respectively. These numbers have been derived from the result output data sheet of a Pascal 440 mercury intrusion porosimeter in a straightforward manner. The results indicate that as curing time increased from 1 to 7 days, there was a decrease in pore radii attributed to chemical reactions. While the average pore radii in mixes with SBA were higher than the control mix, total porosity was reduced in SCC with SBA compared to SCC-CM after 7 days. This reduction was attributed to the formation of CSH gel through pozzolanic reactions, the filler effect of SBA filling gaps between particles, and the irregular particle shape promoting a denser microstructure (Zhang et al., 2020a). However, it is important to note that the microstructure may be influenced by the chemical and physical properties of SBA (Memon et al., 2022). The link between pore size and the amount of SCC pastes formulations that were intruded is shown in Figs. 26, 27 and 28. The threshold diameters were roughly determined by performing a visual assessment of curves that had been produced in Microsoft Office Excel Sheets as shown and marked with arrows. In Figs. 27 and 28, it was observed that the intruded volume was decreased as the curing time increased compared to the control mix. Figs. 29, 30 and 31 demonstrate the distribution of pore radii with respect to intruded volume.

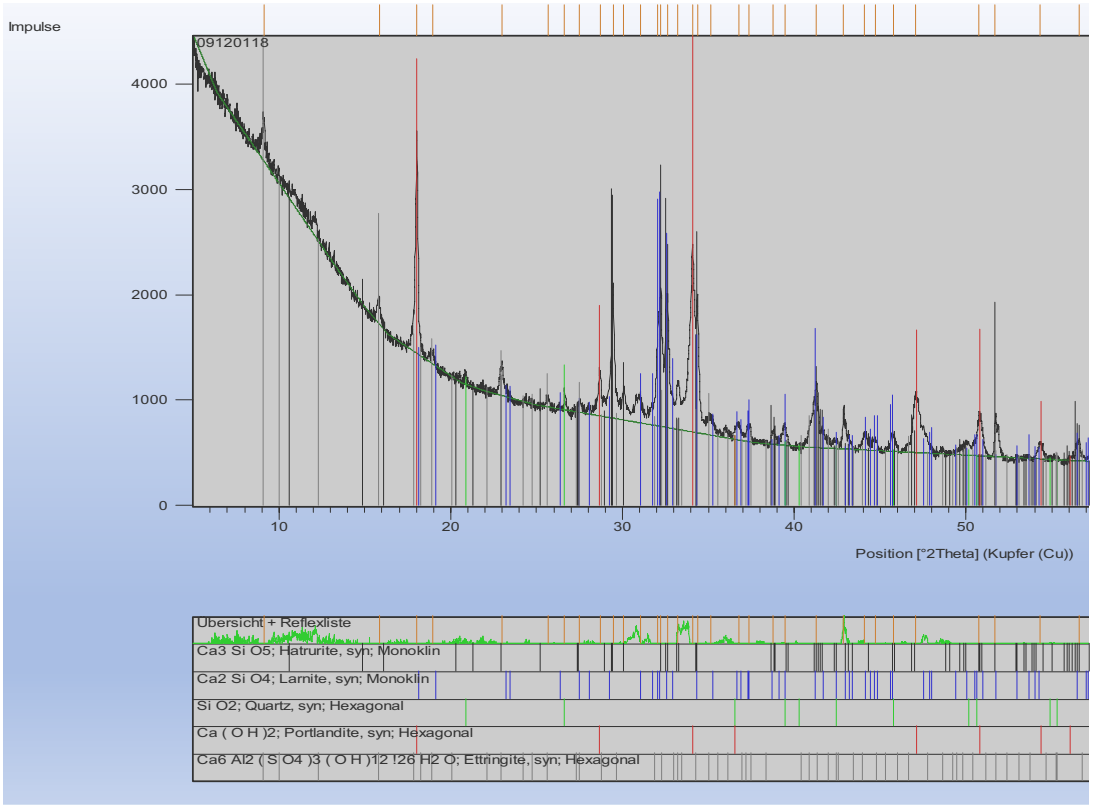

Fig. 12 XRD examination of the SCC-control mix sample at the age of 7 days, identifying the following main phases: alite, belite, ferrite, quartz, and ettringite

3.9 Compressive Strength

Fig. 32 exhibits the results of compressive strength tests conducted after 7, 28, and 56 days, respectively. SCC-15B was able to generate the highest compressive strength of 30 MPa after 56 days of curing. In comparison with the control concrete, two mixes, SCC-10B and SCC-15B, demonstrated an increase in their respective strengths. The addition of SBA into SCC can react with the portlandite the main hydration product of OPC and can increase the formation of CSH gel that can potentially denser the microstructure and increase density as discussed in the previous sections. The CSH gel formation is responsible for the strength improvement. According to Channa et al. (2022) and Batool et al. (2020), an optimal proportion of SBA, typically 5 to 10%, can enhance strength and enable structural applications. In addition, combining SBA with other supplementary cementitious materials like rice husk ash can further enhance cementitious mix performance while reducing environmental pollution (Channa et al., 2022). SEM, MIP, and density tests suggest that SBA addition increases strength by forming additional CSH gel through pozzolanic reactions, resulting in a denser microstructure (Thomas et al., 2021c; Zhang et al., 2020a). However, exceeding the optimal SBA dosage reduces compressive strength; for instance, a mix with 20% SBA experienced decreased strength due to unreacted particles (Channa et al., 2022). Even though it included a greater percentage of SBA, the SCC-20B mix had shown a decline in strength. Regardless of whether or not the mixes are within the SCC limitations, greater compressive strengths were achieved after 7, 28, and 56 days in both control concrete and blended mixes (while maintaining a 2% dose of Super Plasticizer). This was the case regardless of whether or not the mixes were blended. Fig. 33 states the trend of the compressive strength graphs with equations.

3.10 Density of SCC

The control concrete reached its maximum density of 2382 kg/m^3 while containing just 2% of the superplasticizer that was required for flowability. Fig. 34 depicts the outcomes of the density test. The density of SCC-15B achieved its maximum value, however, beyond this point, a decline in the graph was noticed owing to a reduction in the amount of reacted SBA powder present. This effect leads the SCC mix to a decrease in its compressive strength value. SCC-15B successfully attained the maximum density, which comprised of 2% of the dose of

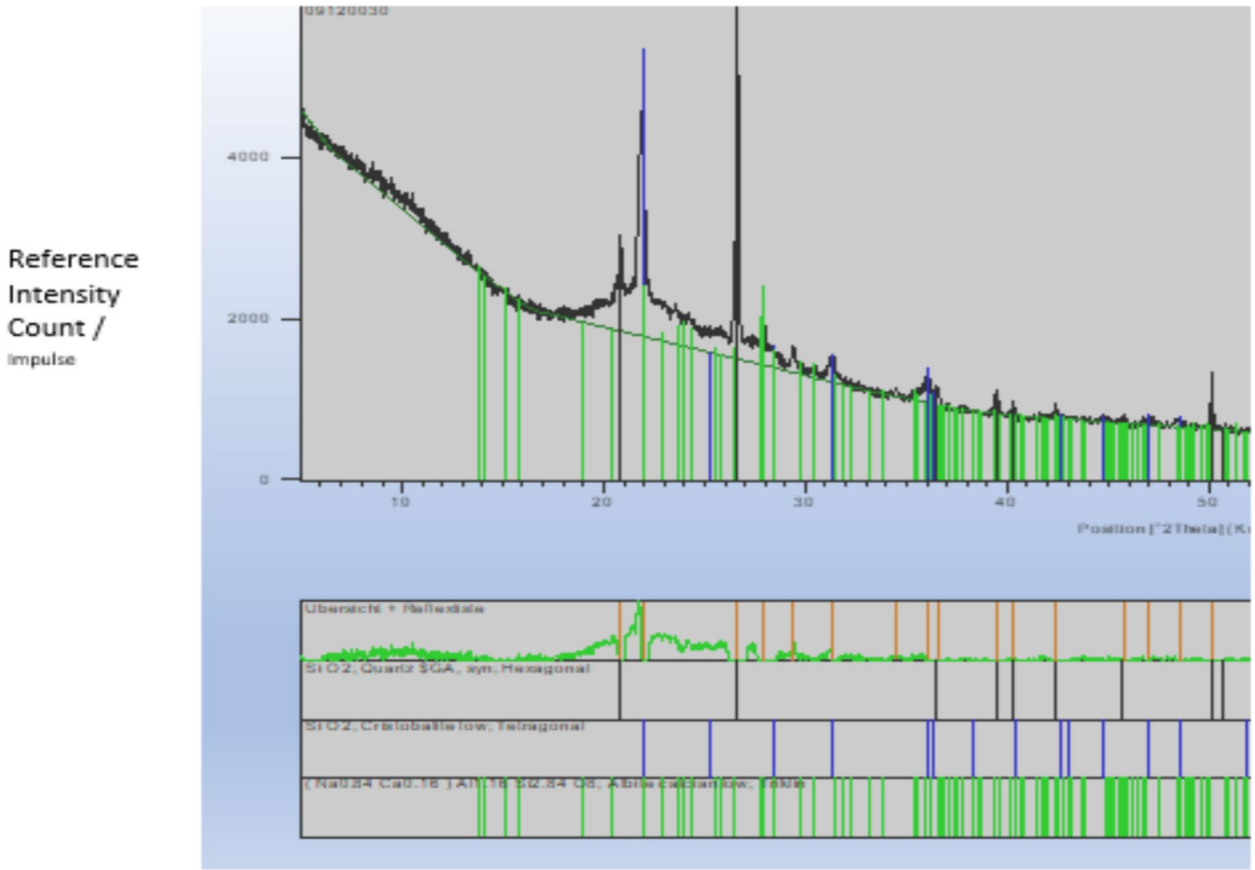

Fig. 13 XRD examination of the main phases found in bagasse ash particles. These phases include quartz, cristobalite, and feldspar (Albite)

superplasticizer. The decline in the graph that occurred after the value of 15% BA was surpassed showed that bagasse ash filled the pores, leaving no gaps when the value of 15% BA was applied (Thomas et al., 2021c). This is because the density is a function of the specific gravity of bagasse ash, and when other factors such as the cement content and the water content are held constant, this becomes apparent. After filling all of the pores in the concrete with SBA, the density fell because the specific gravity of bagasse ash is lower than that of cement resulting in a decline in density.

3.11 Cost Analysis

Table 5 presents a cost analysis of control mix (SCC-CM) and the mix containing 15% SBA (SCC-15B). The cost analysis is done according to the Pakistani rupees and local market rate of ingredients based on the market rate schedule of Pakistan. The addition of 15% SBA in can reduced the overall cost of concrete by 79.24% compared to the control mix. This reduction in cost demonstrates the economic benefit of incorporating bagasse ash in the concrete mixture.

This cost analysis compares two concrete mixtures: control mix (SCC-CM) and SCC with 15% SBA (SCC-15B). The table breaks down the cost of materials per kilogram and the total cost for each mixture. Notably, SCC-15B incorporates SBA, obtained at no cost, which significantly reduces the overall material expenses compared to SCC-CM. The cost reduction achieved by using SBA amounts to approximately 79.24%, highlighting the economic advantage of utilizing this additive in concrete production. This analysis underscores the potential for cost savings and resource efficiency through the incorporation of alternative materials like SBA in concrete mixtures.

4 Discussion

The study highlights the potential of using SBA as a VMA to create cost-effective blends of SCC. Incorporating SBA with concrete and superplasticizer components offers economical SCC production, albeit requiring a reduced water-to-binder ratio. Various combinations of SBA and cement yielded different slump flow, L-box, and V-funnel measurements for SCC mixes that meet the European Federation for Specialist Construction Chemicals and

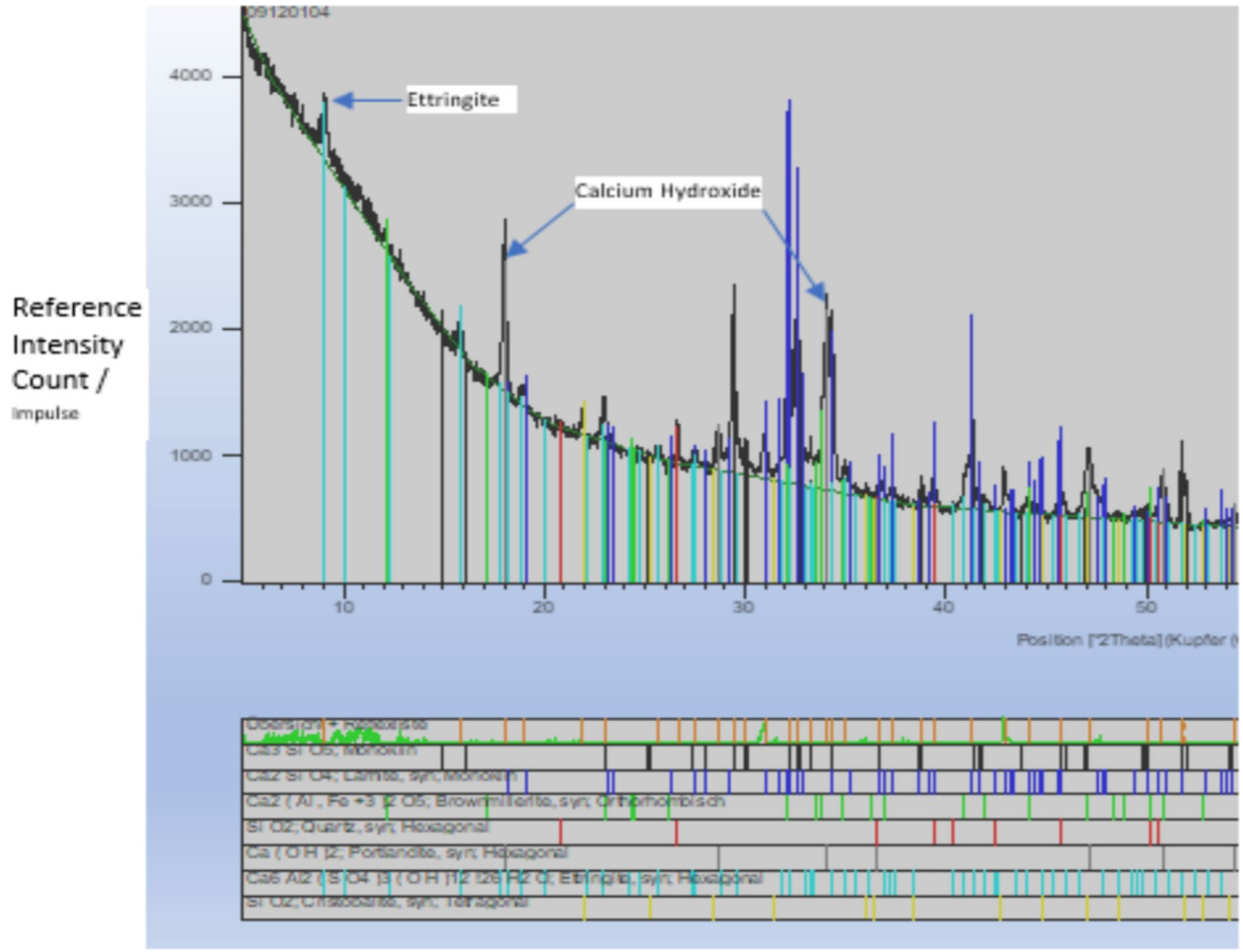

Fig. 14 XRD examination of the SCC-10% bagasse ash mix sample at the age of 1 day, identifying the following main phases: Alite, Belite, Ferrite, Quartz, Portlandite, Ettringite and Cristobalite

Concrete Systems (EFNARC) guidelines. Among the tested combinations, the control concrete and a mix with 5% SBA displayed results within the range specified by the EFNARC, indicating their suitability (Channa et al., 2022). However, some SCC mixes, notably SCC 15B and SCC 20B, surpassed the EFNARC guideline's permissible limits, highlighting the necessity of assessing fresh characteristics before casting. Refining SBA through milling can potentially improve flow properties and packing efficiency. SBA-based SCC exhibited enhanced compressive strength compared to control SCC, attributed to the formation of CSH gel and denser microstructure as discussed in the XRD, SEM, and MIP results. The optimal SCC formulation contained 15% bagasse ash and 2% superplasticizer, achieving a compressive strength of 30 MPa, outperforming SCC-CM. Economically, SCC-15B offered a potential mix proportion for the practical application of infrastructure compared to the control SCC. In addition, the addition of SBA can potentially reduce the high calcination temperature compared to the OPC production (Thomas et al., 2021c). Lastly, combining SBA with other supplementary cementitious materials (SCMs) can enhance specific characteristics of contemporary concretes, potentially improving the overall performance of concrete (Channa et al., 2022).

5 Conclusions

The experimental findings from the examination of fresh and hardened SCC containing SBA as a VMA are analyzed. The following are the conclusive observations:

- The addition of SBA in SCC can mitigate the climate change issue by reducing carbon emissions as well as providing eco-friendly construction materials.
- Incorporating up to 5% SBA can meet EFNARC guidelines and ensure flowable SCC, but higher SBA percentages may decrease flowability due to increased viscosity and friction resistance.

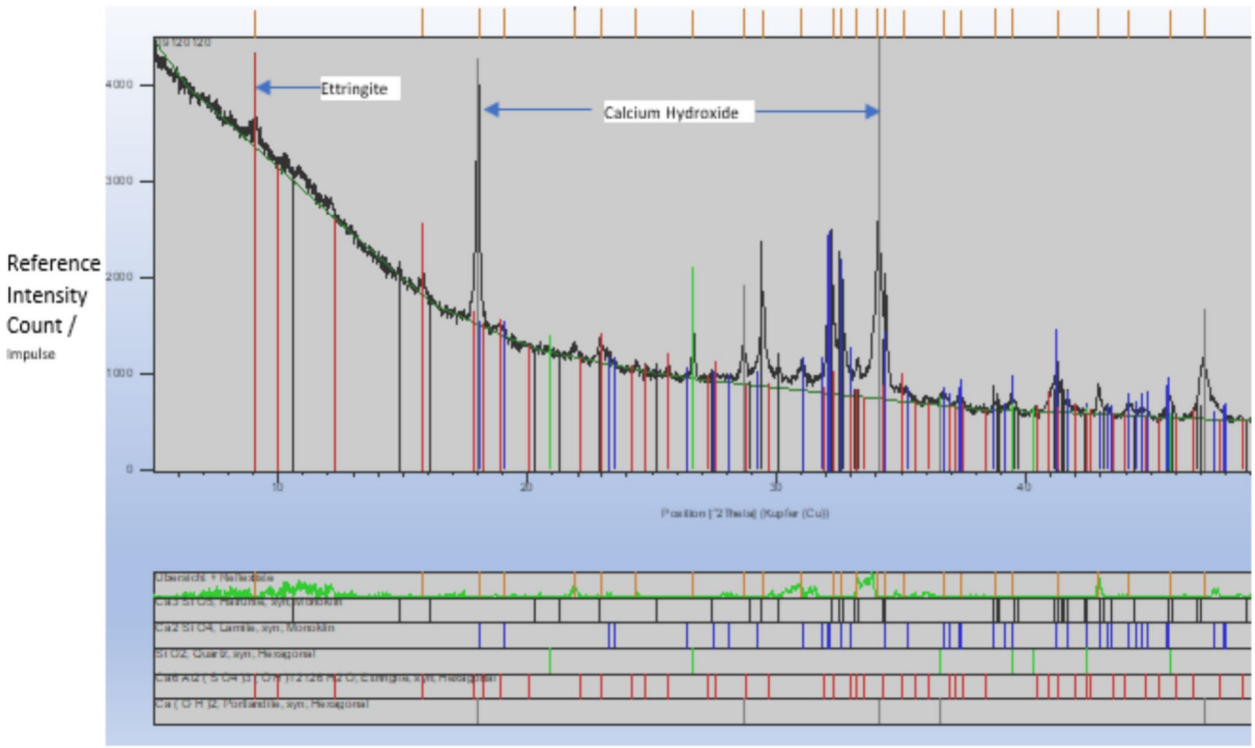

Fig. 15 XRD examination of the SCC-10% bagasse ash mix sample at the age of 7 days, identifying the following main phases: Alite, Belite, Ferrite, Quartz, Portlandite, Ettringite and Cristobalite

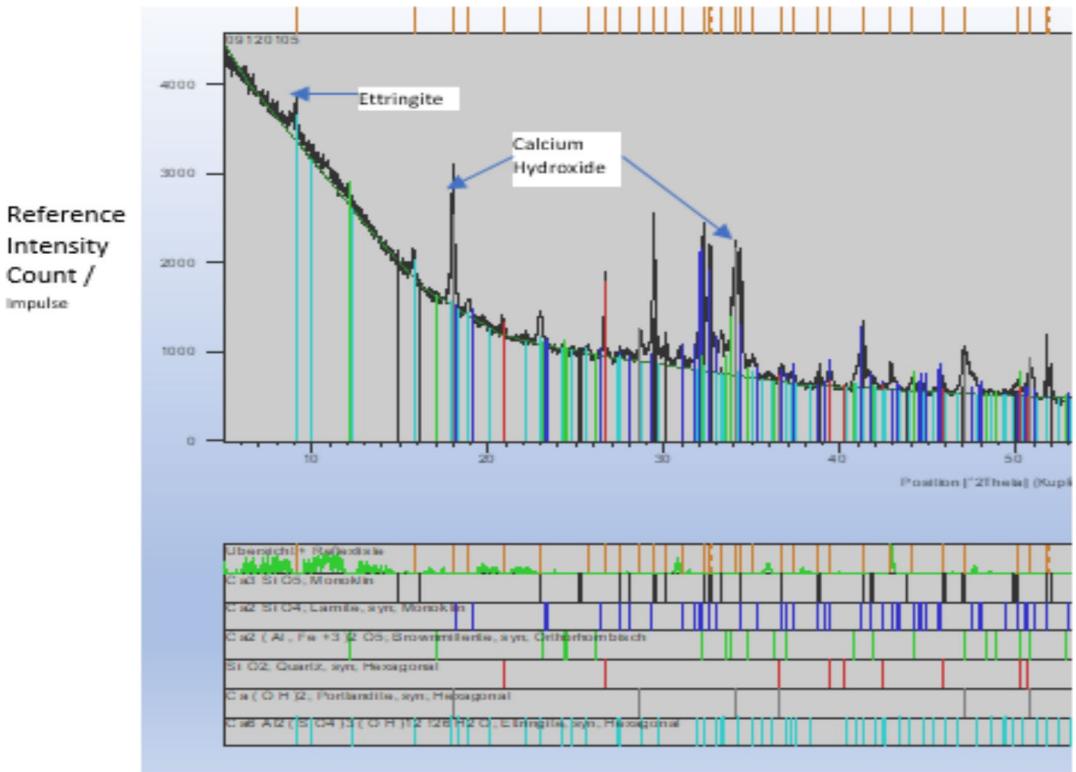

Fig. 16 XRD examination of the SCC-15% bagasse ash mix sample at the age of 1 day, identifying the following main phases: Alite, Belite, Ferrite, Quartz, Portlandite, Ettringite and Cristobalite

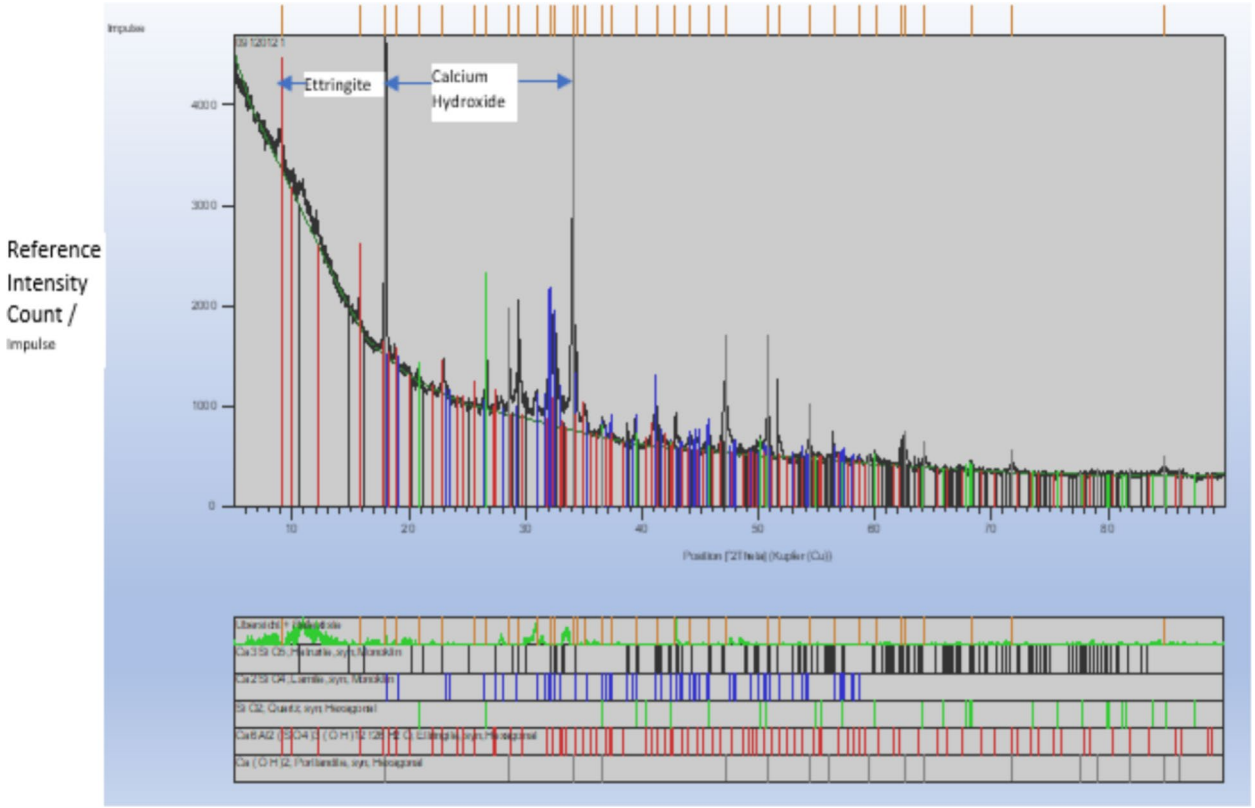

Fig. 17 XRD examination of the SCC-15% bagasse ash mix sample at the age of 7 days, identifying the following main phases: Alite, Belite, Ferrite, Quartz, Portlandite, Ettringite and Cristobalite

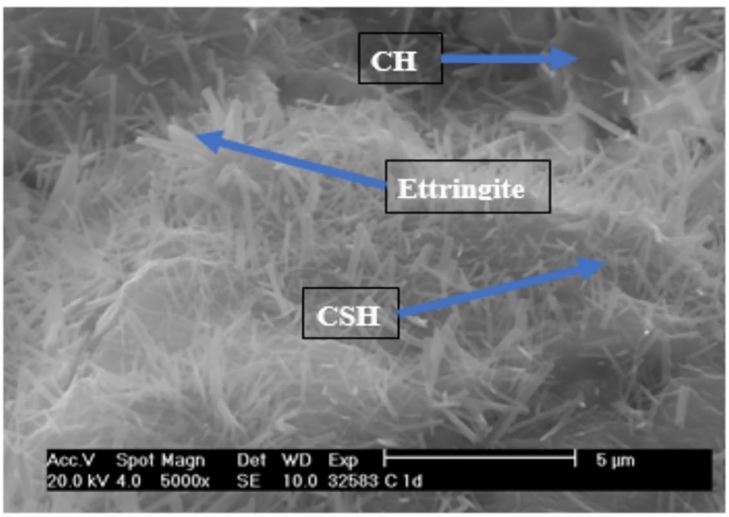

EDAX

Ingredients	Weight %
CaO	53.33
MgO	03.48
Al_2O_3	06.92
SiO_2	21.16
SO_3	09.34
K_2O	02.20
Fe_2O_3	03.57

Fig. 18 EDAX showing percentage weight of ingredients for image of SCC-CM sample at an age of 1 day

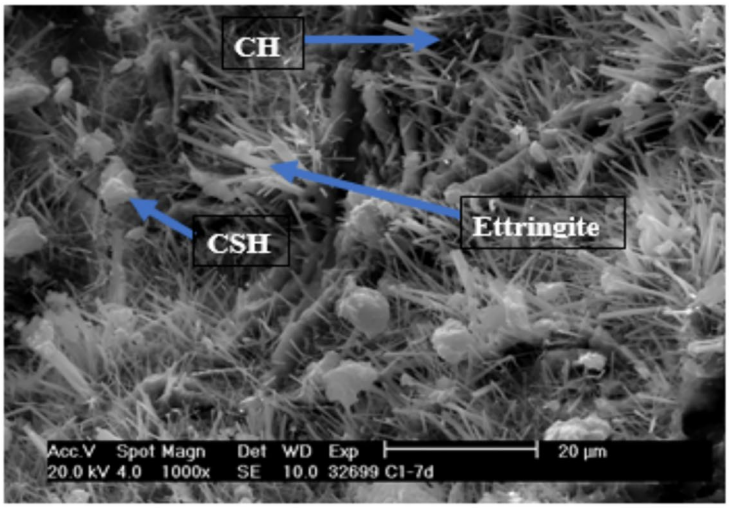

EDAX

Elements	Weight %
CaO	56.62
MgO	01.40
Al_2O_3	11.43
SiO_2	10.78
SO_3	15.44
K_2O	02.05
Fe_2O_3	02.28

Fig. 19 EDAX showing percentage weight of ingredients for image SCC-CM sample at an age of 7 days

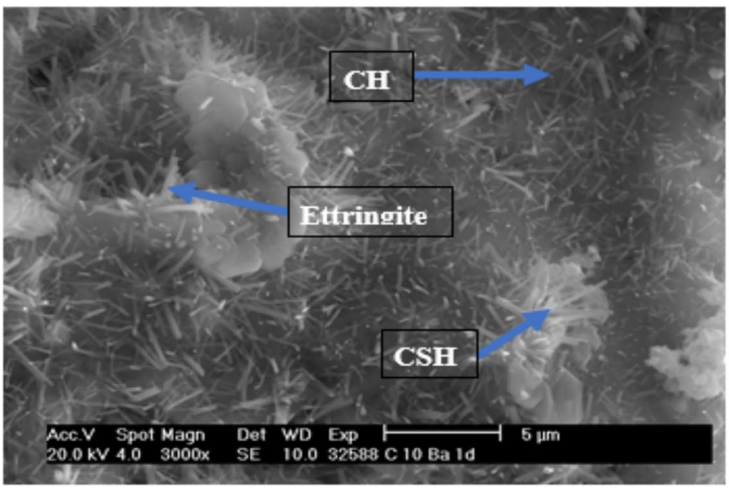

EDAX

Ingredients	Weight %
CaO	59.08
MgO	05.18
Al_2O_3	06.45
SiO_2	15.22
SO_3	07.51
K_2O	01.64
Fe_2O_3	04.92

Fig. 20 EDAX showing percentage weight of ingredients for image of SCC-10B sample at an age of 1 day

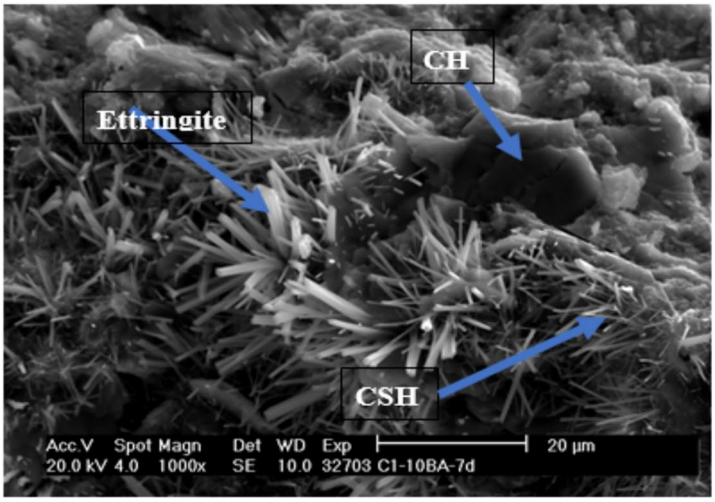

EDAX

Ingredients	Weight (%)
CaO	52.59
MgO	00.66
Al_2O_3	12.08
SiO_2	10.87
SO_3	22.04
K_2O	00.67
Fe_2O_3	01.09

Fig. 21 EDAX showing percentage weight of ingredients for image of SCC-10B sample at an age of 7 days

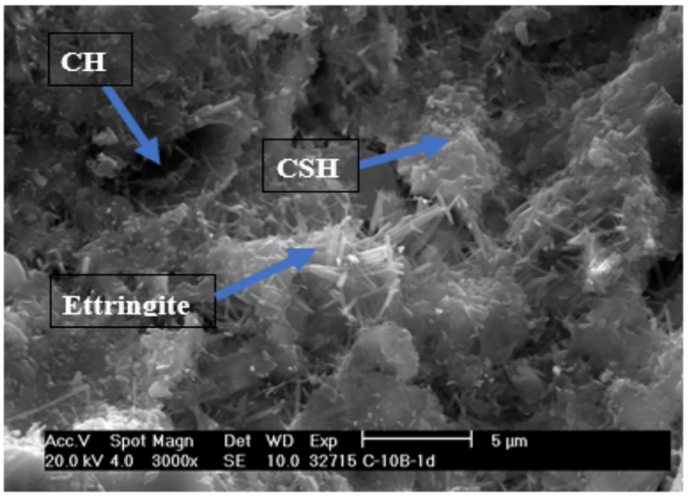

EDAX

Ingredients	Weight %
CaO	50.05
Na_2O	00.36
MgO	02.22
Al_2O_3	05.58
SiO_2	31.24
SO_3	07.43
K_2O	02.12
Fe_2O_3	01.00

Fig. 22 EDAX showing percentage weight of ingredients for image of SCC-15B sample at an age of 1 day

- The optimal compressive strength was observed in the mixture containing 15% SBA, with strength decreasing as the dosage increased. This strength improvement is attributed to denser microstructure, reduced porosity, and potential CSH gel formation within the SCC.
- When comparing the prices of SCC-CM and SCC-15B, a savings of 79.24% was found.

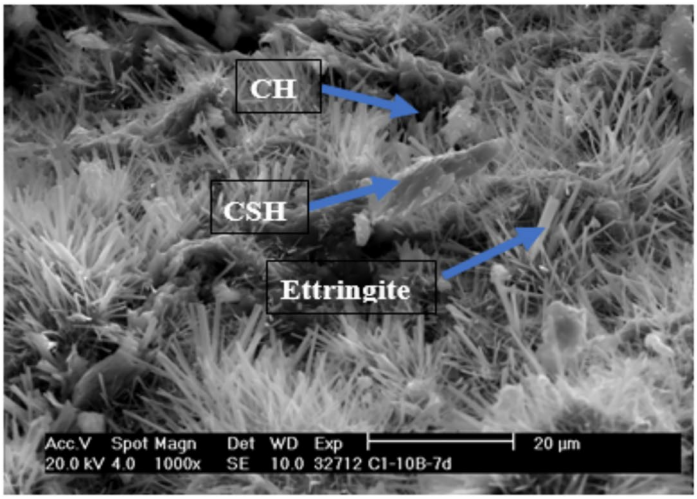

EDAX

Elements	Weight (%)
CaO	50.48
Na_2O	00.27
MgO	00.62
Al_2O_3	16.70
SiO_2	08.40
SO_3	20.74
K_2O	01.21
Fe_2O_3	01.58

Fig. 23 EDAX showing percentage weight of ingredients for image of SCC-15B sample at an age of 7 days

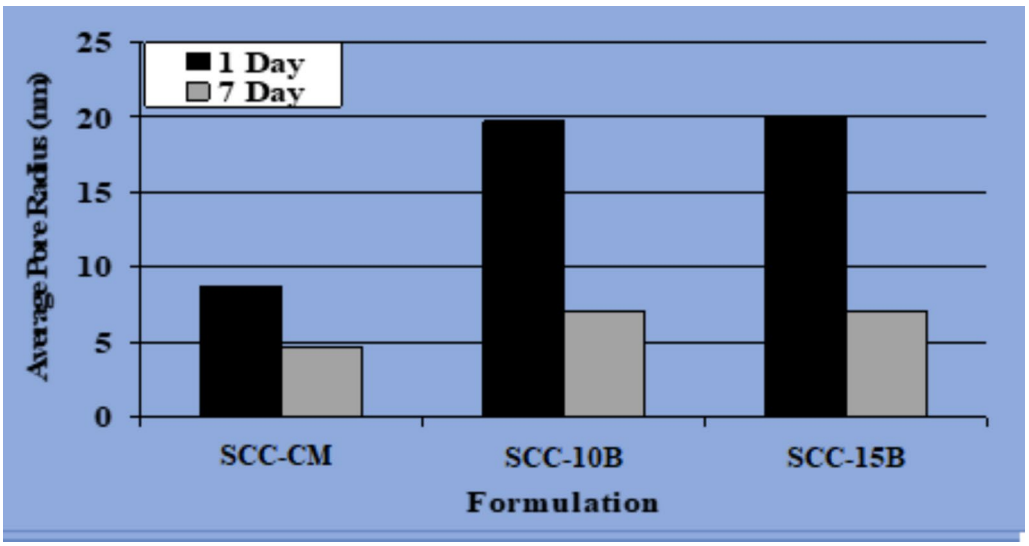

Fig. 24 Average pore width of SCC control and bagasse ash mixes

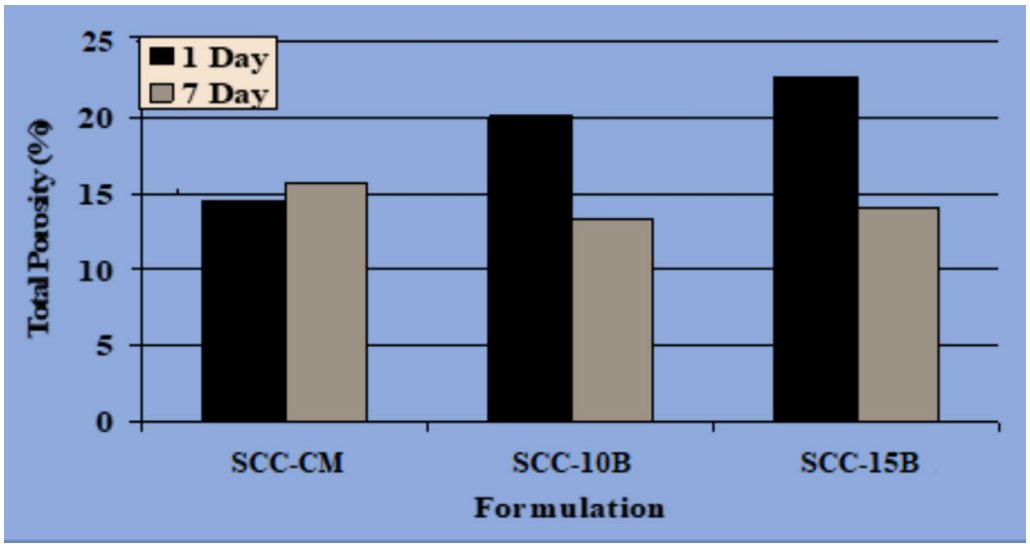

Fig. 25 Total porosity of SCC control and bagasse ash mixes

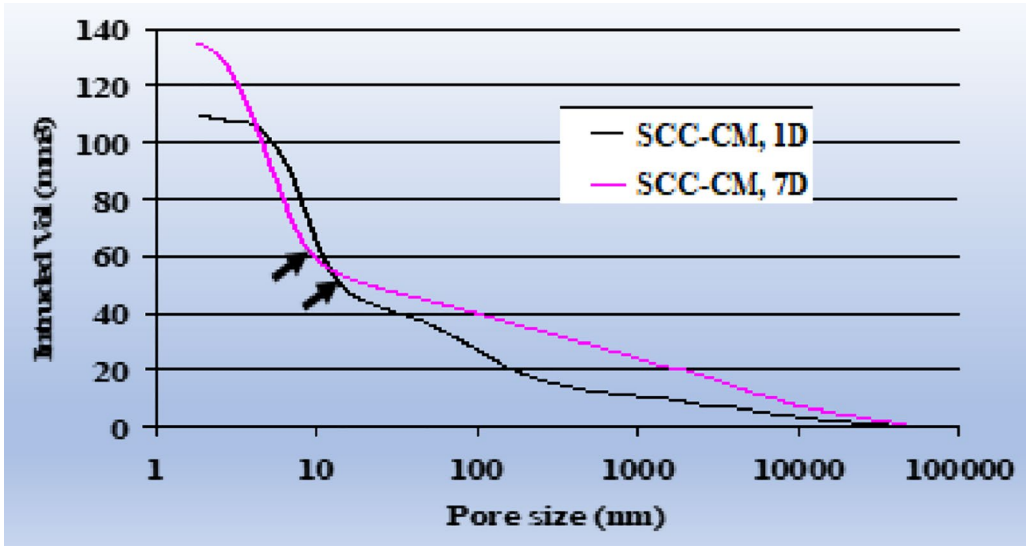

Fig. 26 SCC control mix pore size vs intruded volume curves at specified ages

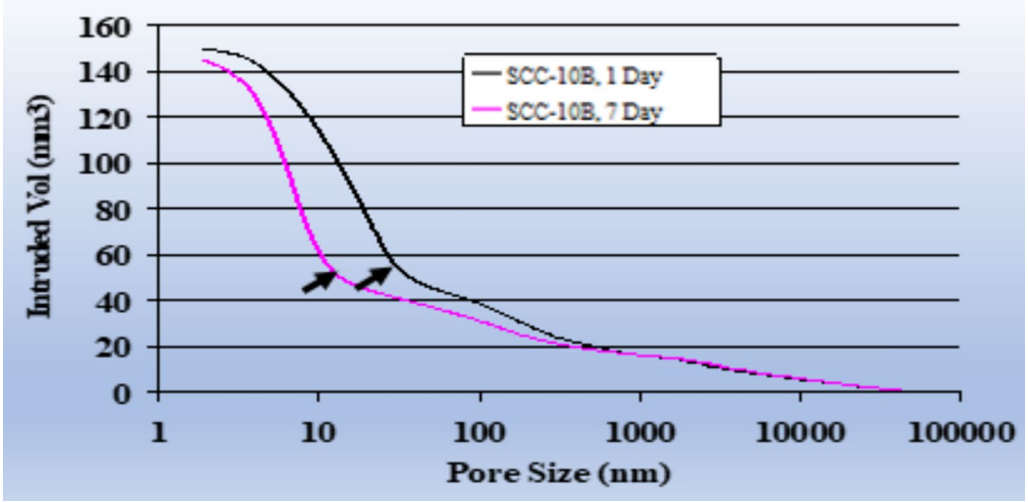

Fig. 27 SCC-10B mix pore size vs intruded volume curves at specified ages

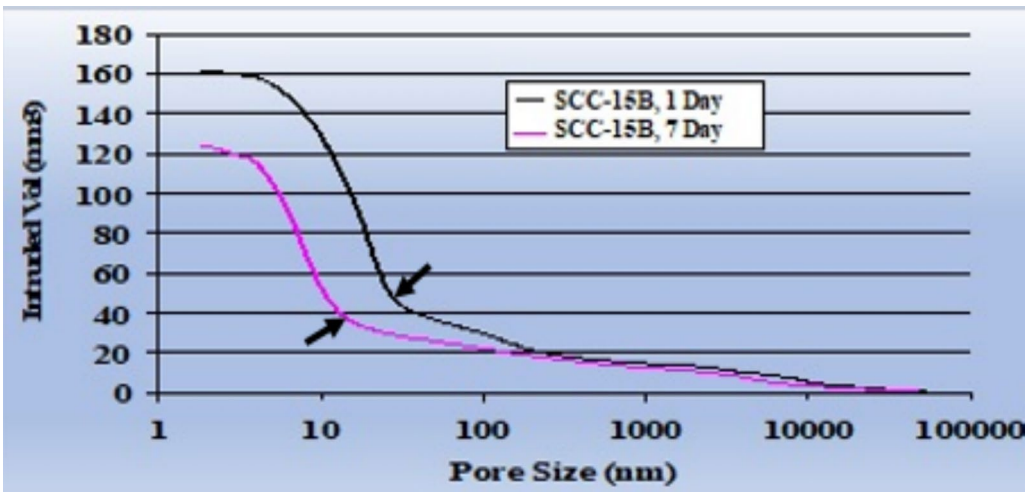

Fig. 28 SCC-15B mix pore size vs intruded volume curves at specified ages

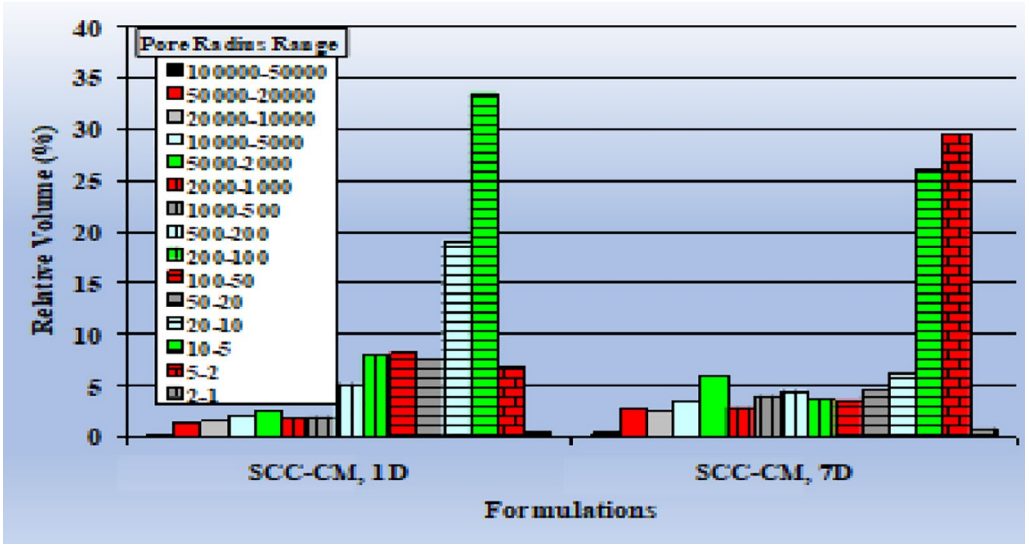

Fig. 29 SCC control mix MIP results pore radi with respect to Intruded Volume

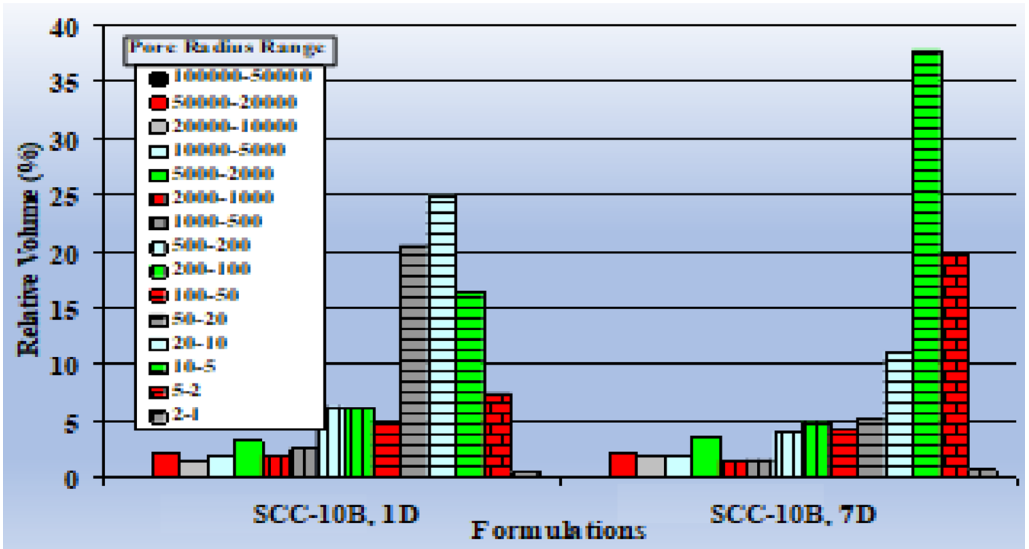

Fig. 30 SCC-10B mix MIP results pore radii with respect to intruded volume

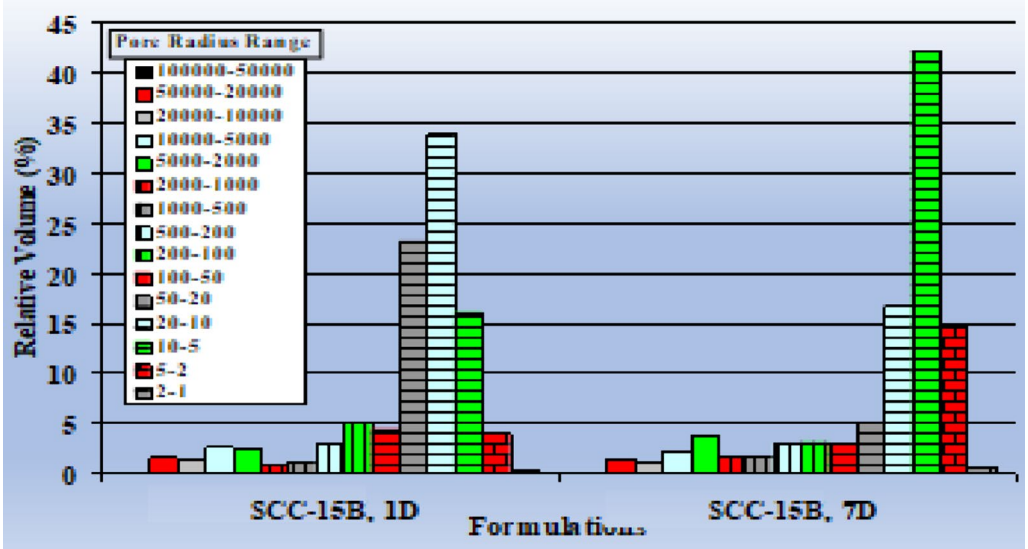

Fig. 31 SCC-15B mix MIP results pore radii with respect to intruded volume

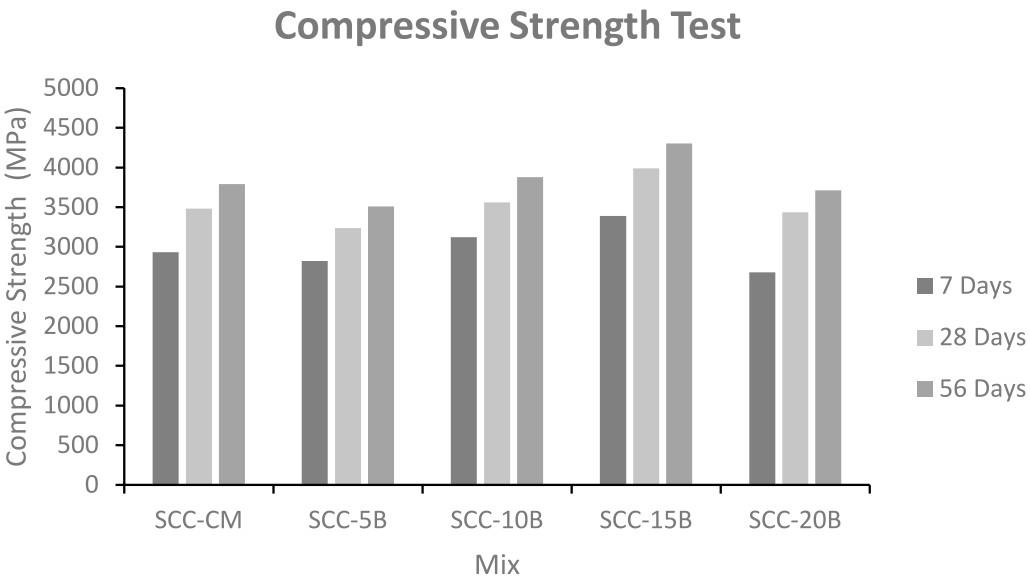

Fig. 32 Compressive strength test results (MPa)

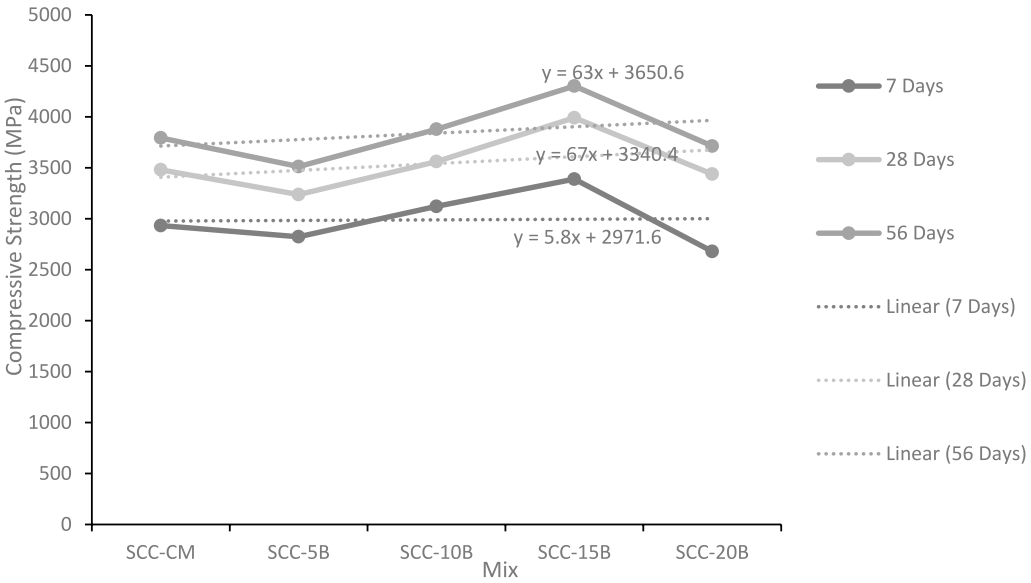

Fig. 33 Trend line for compressive strength (MPa)

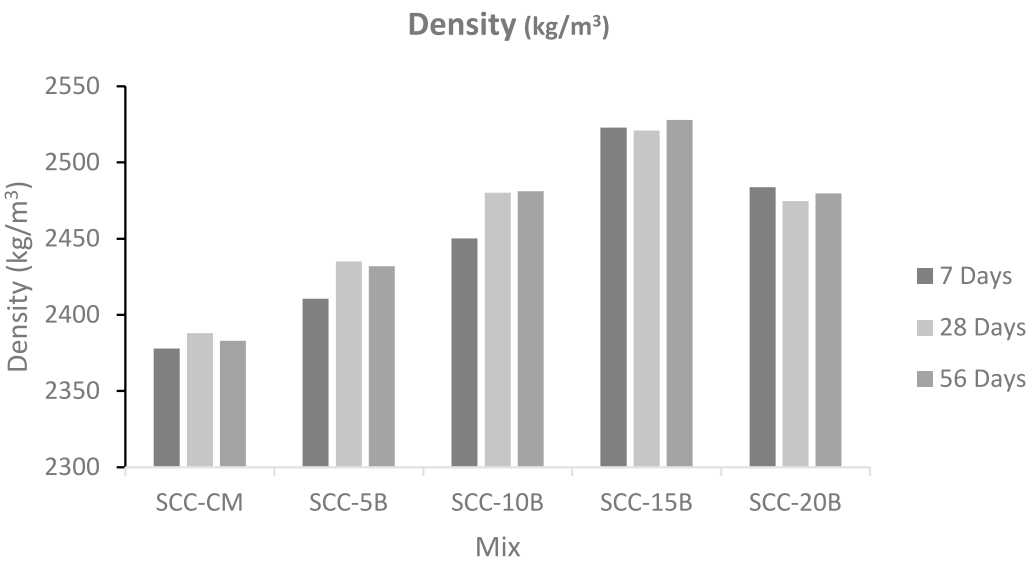

Fig. 34 Density of hardened concrete at 1 day vs SCC mixes of bagasse ash

Table 5 Cost analysis of concrete mixtures with and without SBA as additive

Material	Rate per kg (PKR.)	Control Concrete (SCC-CM)		SCC with bagasse ash (SCC-15B)	
		Quantity (kg)	Amount (Rupees)	Quantity (kg)	Amount (PKR.)
Cement	24.00	43.00	1032.00	36.55	877.20
Coarse aggregate	0.20	75.00	14.85	75.00	14.85
Sand	0.11	65.00	6.83	65.00	6.83
Superplasticizer (Ultra Super Plast 310)	50.00	0.86	43.00	0.86	43.00
Superplasticizer (Viscocrete)	4000.00	0.86	3440.00	–	
Bagasse ash	Free of cost	–	–	6.45	–
Total	–	–	4536.68	–	941.875

Percent reduction in cost = 79.24%

Author contributions
Usman Amjad contributed to the conceptualization, resources, methodology, formal analysis, investigation, writing—original draft, writing—review and editing, and overall coordination of the research project. Muhammad Sarir was involved in the supervision, investigation, methodology, writing—review and editing, and significantly involvedment in experimental design and data interpretation. Diyar Khan participated in writing—review and editing, funding acquisition, and formal analysis and made substantial contribution to the overall research framework and critical review of the manuscript and major contribution to data collection and analysis. Inzimam Ul Haq assisted in the investigation, formal analysis, writing—original draft and writing—review and editing. Muhammad Wajahat Ali Khawaja and Khalid Mahmood contributed to writing—review and editing.

Data availability
All data used in this research appear in the submitted article.

Declarations

Competing interests
The authors declare no competing interests.

Received: 22 February 2024 Accepted: 5 August 2024
Published online: 01 January 2025

References

Abbas, S., Sharif, A., Ahmed, A., Abbass, W., & Shaukat, S. (2020). Prospective of SBA for controlling the alkali-silica reaction in concrete incorporating reactive aggregates. *Structural Concrete, 21*(2), 781–793.
ACI Committee 211. (1991). Standard practice for selecting proportions for normal, heavyweight and mass concrete. American Concrete Institute.
Akkarapongtrakul, A., Julphunthong, P., & Nochaiya, T. (2017). Setting time and microstructure of Portland cement-bottom ash–SBA pastes. *Monatshefte Für Chemie, 148*, 1355–1362.
Akram, M., Ali, T., Memon, N. A., & Khahro, S. H. (2017). Causal attributes of cost overrun in construction projects of Pakistan. *International Journal of Civil Engineering and Technology., 8*(6), 477–483.
Akram, T., Memon, S. A., & Obaid, H. (2009). Production of low cost self compacting concrete using bagasse ash. *Construction and Building Materials, 23*(2), 703–712.
Alberti, M., Enfedaque, A., Gálvez, J., & Cortez, A. (2020). Optimisation of fibre reinforcement with a combination strategy and through the use of self-compacting concrete. *Construction and Building Materials, 235*, 117289.
Ali, A., Uz Zaman Khan, Q., Saqib Mehboob, S., Tayyab, A., Hayyat, K., Khan, D., Ul Haq, I., & Bux Alias Imran Latif Qureshi, Q. (2024). Enhancing multi-objective mix design for GGBS-based geopolymer concrete with natural mineral blends under ambient curing: A Taguchi-Grey relational optimization. *Ain Shams Engineering Journal, 15*(5), 102708. https://doi.org/10.1016/j.asej.2024.102708
Ali, K., Amin, N. U., & Shah, M. T. (2009). Physicochemical study of bagasse and bagasse ash from the sugar industries of NWFP, Pakistan and its recycling in cement manufacturing. *Journal of the Chemical Society of Pakistan, 31*(3), 375–378.
Ali, K., Noor-ul-Amin, Shah, T., Saeed-ur-Rehman. (2010). Physico-chemical study of bagasse and bagasse ash from the sugar industries of NWFP Pakistan and remediation of environmental problems caused by refused bagasse ash. In: Gökçekus, H., Türker, U., LaMoreaux, J. (eds) Survival and sustainability. Environmental earth sciences. Springer Berlin Heidelberg. https://doi.org/10.1007/978-3-540-95991-5_115
Ameri, F., Shoaei, P., Bahrami, N., Vaezi, M., & Ozbakkaloglu, T. (2019). Optimum rice husk ash content and bacterial concentration in self-compacting concrete. *Construction and Building Materials, 222*, 796–813.
American Society for Testing and Materials (Filadelfia), P. (2019). ASTM C136/C136M-19: Standard test method for sieve analysis of fine and coarse aggregates. ASTM.
Anjos, M. A., Araujo, T. R., Ferreira, R. L., Farias, E. C., & Martinelli, A. E. (2020). Properties of self-leveling mortars incorporating a high-volume of sugar cane bagasse ash as partial Portland cement replacement. *Journal of Building Engineering, 32*, 101694.
ASTM, C. (2003). (ASTM). Standard specification for concrete aggregates. *Phila. PA Am. Soc. Test. Mater.*
ASTM. (2005). 39/C 39M standard test method for compressive strength of cylindrical concrete specimens. Annual Book ASTM Standard. 4.
ASTM, A. S. A. (2008). C131/C131M: Standard test method for resistance to degradation of small-size coarse aggregate by abrasion and impact in the Los Angeles Machine. ASTM.
ASTM C1723-16. (2016). Standard guide for examination of hardened concrete using scanning electron microscopy.
ASTM C150/C150M-20. (2020). Standard specification for Portland cement. *Tech. Rep. ASTM Int. West Conshohocken PA*.
ASTM D4404. (2004). Standard test for determination of pore volume distribution of soil and rock by MIP.
Athira, G., Bahurudeen, A., Sahu, P. K., Santhanam, M., Nanthagopalan, P., & Lalu, S. (2020). Effective utilization of sugar industry waste in Indian construction sector: A geospatial approach. *Journal of Material Cycles and Waste Management., 22*, 724–736.
Basu, P., Thomas, B. S., Gupta, R. C., & Agrawal, V. (2021a). Properties of sustainable self-compacting concrete incorporating discarded sandstone slurry. *Journal of Cleaner Production, 281*, 125313.
Basu, P., Thomas, B. S., Gupta, R. C., & Agrawal, V. (2021b). Strength, permeation, freeze-thaw resistance, and microstructural properties of self-compacting concrete containing sandstone waste. *Journal of Cleaner Production, 305*, 127090.
Batool, F., Masood, A., & Ali, M. (2020). Characterization of sugarcane bagasse ash as pozzolan and influence on concrete properties. *Arabian Journal*

for Science and Engineering, 45(5), 3891–3900. https://doi.org/10.1007/s13369-019-04301-y
Bibi, T., Ali, A., Zhang, J., Naseer, A., & Islam, S. U. (2020). Microscopic analysis of the deleterious effects of ammonium nitrate fertilizer on concrete. *Construction and Building Materials, 249*, 118716.
Channa, S. H., Mangi, S. A., Bheel, N., Soomro, F. A., & Khahro, S. H. (2022). Short-term analysis on the combined use of sugarcane bagasse ash and rice husk ash as supplementary cementitious material in concrete production. *Environmental Science and Pollution Research, 29*(3), 3555–3564. https://doi.org/10.1007/s11356-021-15877-0
Chopra, D., & Siddique, R. (2015). Strength, permeability and microstructure of self-compacting concrete containing rice husk ash. *Biosystems Engineering, 130*, 72–80.
Cordeiro, G. C., Andreão, P. V., & Tavares, L. M. (2019). Pozzolanic properties of ultrafine sugar cane bagasse ash produced by controlled burning. *Heliyon, 5*(10), e02566.
Debadrita Das, T., Saravanan, J., Kunal Bisht, K. I., & Kabeer, S. A. (2022). A review of fresh properties of self-compacting concrete incorporating sugarcane bagasse ash. *Materials Today: Proceedings, 65*, 852–859. https://doi.org/10.1016/j.matpr.2022.03.451
Deepika, S., Anand, G., Bahurudeen, A., & Santhanam, M. (2017). Construction products with SBA binder. *Journal of Materials in Civil Engineering, 29*(10), 04017189.
Diab, A. M., Abd Elmoaty, M., & Aly, A. A. (2016). Long term study of mechanical properties, durability and environmental impact of limestone cement concrete. *Alexandria Engineering Journal, 55*(2), 1465–1482.
EFNARC, F. (2002). Specification and guidelines for self-compacting concrete. *Eur. Fed. Spec. Constr. Chem. Concr. Syst.*
Faria, K., Gurgel, R., & Holanda, J. (2012). Recycling of SBA waste in the production of clay bricks. *Journal of Environmental Management, 101*, 7–12.
Figueiredo, R. L., & Pavía, S. (2020). A study of the parameters that determine the reactivity of SBAes (SCBA) for use as a binder in construction. *SN Applied Sciences., 2*, 1–15.
Gonzalez-Corominas, A., Etxeberria, M., & Poon, C. (2017). Influence of the quality of recycled aggregates on the mechanical and durability properties of high performance concrete. *Waste Biomass Valorization, 8*, 1421–1432.
Hasnain, M. H., Javed, U., Ali, A., & Zafar, M. S. (2021). Eco-friendly utilization of rice husk ash and bagasse ash blend as partial sand replacement in self-compacting concrete. *Construction and Building Materials, 273*, 121753.
He, Z., Shen, A., Lyu, Z., Li, Y., Wu, H., & Wang, W. (2020). Effect of wollastonite microfibers as cement replacement on the properties of cementitious composites: A review. *Construction and Building Materials, 261*, 119920.
Huntzinger, D. N., & Eatmon, T. D. (2009). A life-cycle assessment of Portland cement manufacturing: Comparing the traditional process with alternative technologies. *Journal of Cleaner Production, 17*(7), 668–675.
Hussain, J., Khan, A., & Zhou, K. (2020). The impact of natural resource depletion on energy use and CO2 emission in belt & road initiative countries: A cross-country analysis. *Energy, 199*, 117409.
Jagadesh, P., Ramachandramurthy, A., & Murugesan, R. (2018). Evaluation of mechanical properties of Sugar Cane Bagasse Ash concrete. *Construction and Building Materials, 176*, 608–617.
Jain, A., Chaudhary, S., & Gupta, R. (2022). Mechanical and microstructural characterization of fly ash blended self-compacting concrete containing granite waste. *Construction and Building Materials, 314*, 125480.
Jittin, V., Minnu, S., & Bahurudeen, A. (2021a). Potential of SBA as supplementary cementitious material and comparison with currently used rice husk ash. *Construction and Building Materials, 273*, 121679.
Jittin, V., Minnu, S. N., & Bahurudeen, A. (2021b). Potential of sugarcane bagasse ash as supplementary cementitious material and comparison with currently used rice husk ash. *Construction and Building Materials, 273*, 121679. https://doi.org/10.1016/j.conbuildmat.2020.121679
Khalil, M. J., Aslam, M., & Ahmad, S. (2021). Utilization of SBA as cement replacement for the production of sustainable concrete—A review. *Construction and Building Materials, 270*, 121371.
Khater, H. M. (2013). Effect of silica fume on the characterization of the geopolymer materials. *International Journal of Advanced Structural Engineering., 5*, 1–10.
Larissa, C. A., dos Anjos, M. A., de Sa, M. V., de Souza, N. S., & de Farias, E. C. (2020). Effect of high temperatures on self-compacting concrete with high levels of SBA and metakaolin. *Construction and Building Materials, 248*, 118715.
Le, D.-H., Sheen, Y.-N., & Nguyen, K.-H. (2022). Enhancing compressive strength and durability of self-compacting concrete modified with controlled-burnt SBA-blended cements. *Frontiers of Structural and Civil Engineering, 16*(2), 161–174.
Lyu, Z., Shen, A., Mo, S., Chen, Z., He, Z., Li, D., & Qin, X. (2020). Life-cycle crack resistance and micro characteristics of internally cured concrete with superabsorbent polymers. *Construction and Building Materials, 259*, 119794. https://doi.org/10.1016/j.conbuildmat.2020.119794
Lyu, Z., Shen, A., Wang, W., Lin, S., Guo, Y., & Meng, W. (2021). Salt frost resistance and micro characteristics of polynary blended concrete using in frost areas. *Cold Regions Science and Technology, 191*, 103374. https://doi.org/10.1016/j.coldregions.2021.103374
Madlool, N. A., Saidur, R., Hossain, M. S., & Rahim, N. (2011). A critical review on energy use and savings in the cement industries. *Renewable and Sustainable Energy Reviews, 15*(4), 2042–2060.
Memon, S. A., Javed, U., Shah, M. I., & Hanif, A. (2022). Use of processed sugarcane bagasse ash in concrete as partial replacement of cement: Mechanical and durability properties. *Buildings, 12*(10), 1769. https://doi.org/10.3390/buildings12101769
Mo, K. H., Alengaram, U. J., Jumaat, M. Z., Yap, S. P., & Lee, S. C. (2016). Green concrete partially comprised of farming waste residues: A review. *Journal of Cleaner Production, 117*, 122–138.
Mohamad, N., Muthusamy, K., Embong, R., Kusbiantoro, A., & Hashim, M. H. (2022). Environmental impact of cement production and Solutions: A review. *Materials Today: Proceedings, 48*, 741–746.
MolinFilho, R. G. D., et al. (2019). Self-compacting mortar with SBA: development of a sustainable alternative for Brazilian civil construction. *Environment, Development and Sustainability., 21*, 2125–2143.
Moretti, J. P., Nunes, S., & Sales, A. (2018). Self-compacting concrete incorporating SBA. *Construction and Building Materials, 172*, 635–649.
Muthandi, A., & Banupriya, A. S. (2021). Production of self-compacting concrete with fly ash using bagasse ash as fine aggregate. *Iranian Journal of Science and Technology, Transactions of Civil Engineering, 46*(3), 2187–2200. https://doi.org/10.1007/s40996-021-00719-3
Pacheco-Torgal, F. (2017). High tech startup creation for energy efficient built environment. *Renewable and Sustainable Energy Reviews, 71*, 618–629.
SaadAgwa, I., Zeyad, A. M., Tayeh, B. A., Adesina, A., de Azevedo, A. R. G., Amin, M., & Hadzima-Nyarko, M. (2022). A comprehensive review on the use of sugarcane bagasse ash as a supplementary cementitious material to produce eco-friendly concretes. *Materials Today: Proceedings., 65*, 688–696. https://doi.org/10.1016/j.matpr.2022.03.264
Sidiq, A., Gravina, R. J., Setunge, S., & Giustozzi, F. (2020). High-efficiency techniques and micro-structural parameters to evaluate concrete self-healing using X-ray tomography and Mercury Intrusion Porosimetry: A review. *Construction and Building Materials, 252*, 119030.
"SIka Viscocrete 20HE," Sika® ViscoCrete®-20 HE High Range Water Reducer / Superplasticiser. https://pak.sika.com/en/construction/concrete-technology/ready-mixed-concrete-admixtures/ultra-high-rangewaterreducers/sika-viscocrete-20he.html
Soltanzadeh, F., Emam-Jomeh, M., Edalat-Behbahani, A., & Soltan-Zadeh, Z. (2018). Development and characterization of blended cements containing seashell powder. *Construction and Building Materials, 161*, 292–304.
Stafford, F. N., Raupp-Pereira, F., Labrincha, J. A., & Hotza, D. (2016). Life cycle assessment of the production of cement: A Brazilian case study. *Journal of Cleaner Production, 137*, 1293–1299.
Standard, A. (2006). Standard test method for density, absorption, and voids in hardened concrete. *ASTM Standard C*, 642.
Standard, A. (2009). C1621/C1621M-09b. *Stand. Test Method Passing Abil. Self-Consol. Concr. J-Ring West Conshohocken PA ASTM Int.*
Thomas, B. S., et al. (2021b). SBA as supplementary cementitious material in concrete—A review. *Materials Today Sustainability., 15*, 100086.
Thomas, B. S., Yang, J., Bahurudeen, A., Abdalla, J. A., Hawileh, R. A., Hamada, H. M., Nazar, S., Jittin, V., & Ashish, D. K. (2021c). Sugarcane bagasse ash as supplementary cementitious material in concrete—A review. *Materials Today Sustainability., 15*, 100086. https://doi.org/10.1016/j.mtsust.2021.100086
Thomas, B. S., Yang, J., Mo, K. H., Abdalla, J. A., Hawileh, R. A., & Ariyachandra, E. (2021a). Biomass ashes from agricultural wastes as supplementary cementitious materials or aggregate replacement in cement/

geopolymer concrete: A comprehensive review. *Journal of Building Engineering., 40*, 102332.
Tibbetts, C. M., Tao, C., Paris, J. M., & Ferraro, C. C. (2020). Mercury intrusion porosimetry parameters for use in concrete penetrability qualification using the Katz-Thompson relationship. *Construction and Building Materials, 263*, 119834.
Tripathy, A., & Acharya, P. K. (2022). Characterization of bagasse ash and its sustainable use in concrete as a supplementary binder—A review. *Construction and Building Materials, 322*, 126391.
Ul Haq, I., Elahi, A., Nawaz, A., Shah, S. A. Q., & Ali, K. (2022). Mechanical and durability performance of concrete mixtures incorporating bentonite, silica fume, and polypropylene fibers. *Construction and Building Materials, 345*(February), 128223. https://doi.org/10.1016/j.conbuildmat.2022.128223
Valderrama, C., Granados, R., Cortina, J. L., Gasol, C. M., Guillem, M., & Josa, A. (2012). Implementation of best available techniques in cement manufacturing: A life-cycle assessment study. *Journal of Cleaner Production, 25*, 60–67.
Xu, Q., Ji, T., Gao, S.-J., Yang, Z., & Wu, N. (2018). Characteristics and applications of sugar cane bagasse ash waste in cementitious materials. *Materials, 12*(1), 39.
Yadav, A. L., Sairam, V., Muruganandam, L., & Srinivasan, K. (2020). An overview of the influences of mechanical and chemical processing on sugarcane bagasse ash characterisation as a supplementary cementitious material. *Journal of Cleaner Production, 245*, 118854. https://doi.org/10.1016/j.jclepro.2019.118854
Zareei, S. A., Ameri, F., & Bahrami, N. (2018). Microstructure, strength, and durability of eco-friendly concretes containing SBA. *Construction and Building Materials, 184*, 258–268.
Zeb, K., Ali, Y., & Khan, M. W. (2018). Factors influencing environment and human health by cement industry: Pakistan a case in point. *Management of Environmental Quality: an International Journal, 30*(4), 751–767.
Zhang, P., Liao, W., Kumar, A., Zhang, Q., & Ma, H. (2020a). Characterization of sugarcane bagasse ash as a potential supplementary cementitious material: Comparison with coal combustion fly ash. *Journal of Cleaner Production., 277*, 123834. https://doi.org/10.1016/j.jclepro.2020.123834
Zhang, S., Cao, K., Wang, C., Wang, X., Wang, J., & Sun, B. (2020b). Effect of silica fume and waste marble powder on the mechanical and durability properties of cellular concrete. *Construction and Building Materials, 241*, 117980.

Publisher's Note

Engr. Usman Amjad is an accomplished academic professional serving as an Assistant Professor in the Department of Civil Engineering at Abasyn University, Peshawar, Pakistan. With over 12 years of experience in teaching and research, he has established himself as a prominent figure in the field of civil engineering education. Engr. Amjad's expertise extends beyond traditional teaching. He is a certified Master Trainer in Outcome-Based Education (OBE), having earned this prestigious certification through the United States Education Foundation and the University of Kentucky. This certification underscores his commitment to enhancing educational practices and outcomes in his field. Throughout his career, Engr. Amjad has been dedicated to advancing civil engineering education and contributing to the academic community through his extensive experience and innovative teaching methodologies.

Muhammad Sarir is a faculty member in the Department of Civil Engineering at the International Islamic University, Islamabad, Pakistan. He holds a B.Sc. in Civil Engineering from UET Peshawar and a Master's in Civil Engineering with a focus on highway materials. He specializes in construction materials and sustainable practices, with significant contributions to research in innovative materials for concrete and asphalt.

Diyar Khan is currently a fast-track PhD student in the Faculty of Transport and Aviation Engineering, Silesian University of Technology. His research scope covers transport engineering focused on the noise and vibration, classification of vibroacoustic scenes in transport and civil engineering focused on road construction materials and concrete.

Inzimam Ul Haq is doing PhD in Departmenmt of civil and environmental engineering at KAIST, South Korea. He completed his BSc and MSc civil engineering from University of Engineering and Technology Peshawar and University of Engineering and Technology Taxila, Pakistan, respectively. His research work focuses on cement and concrete material particularly designing a smart and sustainable construction materials for construction of infrastructure and additionally, decarbonizing cement and construction industry by reducing carbon emissions and permanently storing the carbon dioxide in it. Furthermore, strengthening and retrofitting of new and old structures is a part of his previous research work.

Muhammad Wajahat Ali Khawaja is a faculty member in the Department of Civil Engineering at Abasyn University, Peshawar. He specializes in civil engineering with a focus on construction materials and structural engineering. His expertise and contributions are well recognized within the field, and he is actively involved in both teaching and research.

Khalid Mahmood is a faculty member in the Department of Civil Engineering at Abasyn University, Peshawar. He specializes in civil engineering, focusing on structural analysis and construction materials, Khalid Mahmoodand is actively engaged in teaching and research, contributing to advancements in the field through his expertise and academic work.